DRUG REPURPOSED PERPHENAZINE ASSESSMENT FOR HEAD AND NECK CANCER TREATMENT IN VITRO



UNIVERSITY OF BIRMINGHAM

By

Xiaoyu Su

A Thesis submitted to the University of Birmingham for the degree of MRes in Cancer and Genomics.

Word Count:11,926

March 2021

This project was carried out under the supervision of:

Prof. Hisham Mehanna

Dr. Nikolaos Batis

UNIVERSITY OF
BIRMINGHAM

University of Birmingham Research Archive

e-theses repository

This unpublished thesis/dissertation is copyright of the author and/or third parties. The intellectual property rights of the author or third parties in respect of this work are as defined by The Copyright Designs and Patents Act 1988 or as modified by any successor legislation.

Any use made of information contained in this thesis/dissertation must be in accordance with that legislation and must be properly acknowledged. Further distribution or reproduction in any format is prohibited without the permission of the copyright holder.

Table of Contents

1.Abstract……..……-4
2.Introduction…. …….……-5
2.1 Introduction of cancer……..……-5
2.2 Head and neck cancer……..……..-7
2.2.1 Overview……..……..-7
2.2.2 Aetiology…….……..…-8
2.2.3 Molecular biology of head and neck cancer…….…..-10
2.3 Current trend in Cancer drug discovery……..…….…….....-12
2.4 Cancer Drug Repurposing…….....-14
2.5 Perphenazine……..…….....-15
2.5.1 Perphenazine in cancer……..……...…..…-16
2.6 AcceleraTED (in InHANSE) ……..……....…-18
2.7 Current Project outline……....…-19
2.8 Hypothesis and Aim……....…-20
3 Methods and Materials…….....-20
3.1 Cell lines and Reagents……..….-20
3.2 AlamarBlue viability Assay……..……..……-22
3.2.1 Perphenazine concentration-response ± 2 μM cisplatin…….. ……..-22
3.2.2 Cisplatin concentration response with perphenazine…….-23
3.3 Clonogenic Cell Survival Assay…….-23
3.4 Apoptosis assay assessed by Annexin V…….-24
3.5 Cell cycle assay……....-25
3.6 Protein Quantification and Expression by Western Blot……-26
3.7 Statistical Analysis……...-28
4. Results…….-29
4.1 Perphenazine decreases cell viability of HNC……-29
4.1.1 Perphenazine concentration-response with ± 2 μM Cisplatin……-29
4.1.2 Cisplatin concentration-response with increasing Perphenazine……-31
4.2 Perphenazine reduces colony-forming ability…….-32
4.3 PPZ induces apoptosis of HNC cell lines……-35
4.4 PPZ alters LC-3 II/LC-3 I expression in HNSCC cell lines……-38
4.5 cell cycle analysis with PPZ treatment HNC cell line…….-41
5. Discussion……-44
5.1 PPZ induces apoptosis in head and neck cancer……..-44
5.2 PPZ increases LC3 expression in head and neck cancer……..-47
5.3 PPZ treatment and cell cycle in head and neck cancer……-47
5.4 PP2A is the potential target of PPZ in head and neck cancer……..-48
5.5 Limitation and opportunity for further study……...…-51

6. Conclusion……...…-53
7. Acknowledgement……...-54
8. Reference…….-55
9. Appendix…….-61

1. Abstract

As the 7th most frequent type of cancer (Bray et al., 2018), head and neck cancer (HNC) is a complex group of cancers located in the upper aerodigestive tract. About 90% of head and neck cancers are squamous cell carcinomas (HNSCC). Despite several treatments for HNC, the patient outcome is still poor. The chemotherapeutic agent cisplatin may be used in combination with radiotherapy as a primary treatment modality or in the adjuvant setting in locally advanced HNSCC. However, the high toxicity and side effects of this treatment seriously impact the quality of life of patients. Thus, repurposing drugs with lower toxicity to improve the effect of standard therapy is timely and necessary. A multistage drug discovery and repurposing platform has been developed by the InHANSE group, called AcceleraTED. According to the initial screening of 1280 FDA-approved drugs from the Prestwick library, perphenazine was identified as a potential drug to target HNC.

Here, I found that perphenazine (PPZ) reduces the viability of HNSCC FaDu and Cal27 cell lines. Thereby, both cancer cell proliferation and death can be affected by PPZ. PPZ inhibits the colony forming ability in a concentration dependent manner in both FaDu and Cal27 cell lines. Apoptosis could also be induced by PPZ.

In addition, I used Western blot immunoreactivity to evaluate the effect and possible mode of action of perphenazine in HNC, but further work is required. My study provides preliminary evidence to support further assessment of the potential therapeutic effect of perphenazine in head and neck cancer cell lines.

2. Introduction

2.1 Introduction of cancer

According to World Health Organization statistics, cancer is the second leading cause of global death. There were 18.1 million new cancer cases diagnosed and 9.6 million deaths worldwide in 2018. This global burden is estimated to rise to 27.5 million new cases by 2040 (Cancer Research UK). Therefore, improving the efficacy of cancer treatment and prevention is becoming an important problem. In Europe, there is 9% of the world population. However, 23.4% of the global cancer cases and 20.3% of the cancer deaths are confirmed in Europe (Bray et al., 2018). It appears that Europe is a high-incidence area of cancer in the world. Ranked higher than two-thirds of Europe, The United Kingdom has an average of ~360,000 new cancer cases from 2014 to 2016, and this number is estimated to continue increasing (Cancer Research UK). In the UK, cancer accounts for more than one in four of all deaths. Due to its high proportion of death, finding novel ways to improve cancer treatment and prevention is imperative.

Cancer is a disease involving abnormal cell proliferation, and distant invasion and metastasis. There are at least six hallmarks of cancer driving tumourigenesis: limitless proliferation ability, growth signal sustainability, inhibition of cell death, growth suppressor insensitivity, cell invasion and metastasis, and sustained angiogenesis (Figure 1) (Hanahan & Weinberg, 2011). Carcinogenesis, a multistep process by which cancers are generated, is the result of error accumulation affecting vital cell regulation pathways. Malignant growth is derived from a single cell, which acquires advanced survival ability and then gains additional changes over its neighbours. In the cancer initiation stage, due to the effect of carcinogenic factors, the normal cell is at risk of becoming malignant with abnormal cell proliferation and differentiation. After multiple genetic changes, the accumulated genetic abnormalites cannot be corrected by cellular DNA-repair mechanisms. A cell gradually loses its self-regulatory function and tends to escape immunological surveillance and finally becomes 'immortalised', which is named the promotion stage. An altered cell takes time to generate a colony and then develop a tumour that will continue to accumulate gene mutation and other cellular changes

resulting from genetic instability. The genetic errors are recognised by DNA damage response (DDR) machinery followed by three different outcomes: DNA repair, cell cycle arrest, and programmed cell death (Liang, Lin, Brunicardi, Goss, & Li, 2009). Naturally, an average $1x10^{3}$ mutations occur per person per day, but the vast majority of mutations do not lead to cancer. However, qualitative, or quantitative changes involving specific genes, especially those in important signalling pathways, lead to loss of normal cellular control functions s. Consequently, cancer development and progression are inevitable if unchecked.

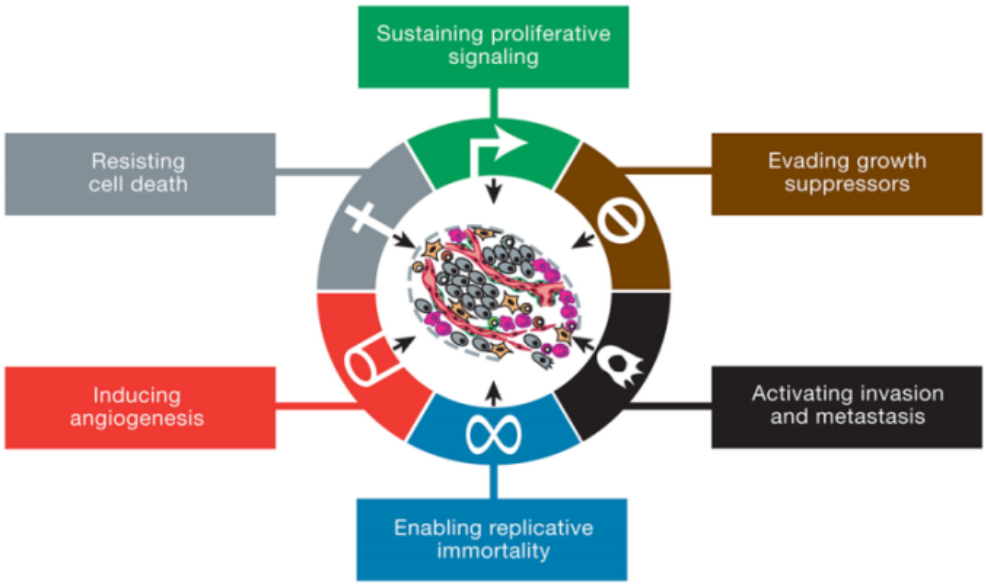


Figure 1. The Hallmarks of Cancer (Hanahan & Weinberg, 2011)

The Diagram includes the six hallmark capabilities as proposed by Hanahan et al.

At the molecular level, two types of genes play a crucial role in malignant development. The first type is oncogenes, which are normal regulatory genes but frequently activated by alteration in their coding sequence in cancer. Based on their protein products, oncogenes can be classified into 5 different types: growth factors, growth factor receptors, non-receptor protein kinase, RAS gene, and nuclear protein-encoding. Their increased expression is involved in important regulation pathways such as cell proliferation and differentiation that

cause cancers. The second type is tumour suppressor genes, encoding proteins proven to have an inhibitory effect in carcinogenesis. The basis of their function in the normal cells is inhibiting cell proliferation and promoting cell differentiation. Alteration or inactivation of these genes generates cell growth or even cancer development. In addition, mismatch repair genes and metabolizing enzyme genes also are relevant to the genesis of cancer. In cancer, genetic changes are common and diverse, which means different cancers may have their own specific genetic changes and altered signalling pathways. Therefore, it is important to concentrate more on the specific genetic mechanisms affecting the cancer of interest - here head and neck cancer.

2.2 Head and Neck Cancer

2.2.1 Overview

According to the global cancer statistics in 2018, Head and Neck Cancer (HNC) is classified as the 7th most frequent type of cancer. More than 880,000 new cases of HNC were diagnosed, accounting for 4.9% of all new cancer cases worldwide (Bray et al., 2018). Lip and oral cavity are the most frequent tumour sites, with more than 350,000 new cases, representing 2% of all cancer incidences in 2018. Ranked second is larynx cancer, representing 1% incidence with associated 1% mortality worldwide (Bray et al., 2018). In the UK, there are approximately 12,000 new HNC occurrences per year, equating to 33 new cases per day (Cancer Research UK). HNC is the 8th most frequent type of cancer in the UK, accounting for 3% of all new cancer cases. Until a decade ago, most HNC cases were diagnosed in the larynx rather than lip and oral cavity in the UK (Cancer Research UK). The frequency of HNC diagnosis in the UK – based on European age-standardised (AS) incidence rates – has increased since the early 1990s. Between 1993-1995 and 2014-2016, British incidence rose by 32% (Cancer Research UK); incidence normally increases with age.

HNC, like most cancer types, is a heterogeneous disease and it is defined as a complex group of cancers located in the upper aerodigestive tract. It encompasses hypopharynx, oropharynx,

lip, oral cavity, nasopharynx, larynx, sinuses, and salivary glands (Mehanna, Paleri, West, & Nutting, 2011). Squamous cell carcinoma, also called epidermoid carcinoma, is by far the most common type of HNC, accounting for over 90%. However, the high pathological consistency of HNC does not simplify clinical treatment; different anatomic sites still have various features requiring different treatments. Treatment of HNC, by any standard, remains complex. As tumours develop from the mouth and ear-nose-throat area, related functions - such as breathing, swallowing, and speaking - are likely to be affected. Also, the relevant safety margin of surgical resection is very limited. No matter which treatment is used - chemotherapy, radiotherapy, or surgery - functional sequelae may result, with an irreversible influence on the quality of life. A more, or equally, efficient clinical therapy with less impairment remains a significant challenge in HNC.

2.2.2 Aetiology

There are many factors associated with HNC development. Tobacco and alcohol consumption are responsible for three-quarters of HNCs, especially head and neck squamous cell carcinoma (HNSCC) (Mehanna et al., 2011). There is a carcinogenic compound in tobacco, acrylonitrile. It can increase oxidative stress and indirectly generate DNA damage, resulting in rising levels of 8-oxo-2'-deoxyguanosine (8-oxo-dG) and formamidopyrimidine in DNA. (Cunningham, Fiebelkorn, Johnson, & Meredith, 2011; Pu, Kamendulis, & Klaunig, 2009). According to the statistics, smoking relates more strongly to laryngeal cancer (Mehanna et al., 2011), and smokeless tobacco mainly causes oral and pharyngeal cancers (oropharyngeal cancer) (Winn, 1992). In terms of alcohol, its consumption is associated with cancers of the pharynx and oral cavity (Mehanna et al., 2011). A pooled analysis of 15 case-control studies relating to alcohol found that, compared with non-drinkers, non-smokers with three or more alcoholic drinks (beer or spirits) a day have double the risk of developing HNC (odds ratio 2.04, 95% confidence interval 1.29 to 3.21) (Hashibe et al., 2007; Purdue et al., 2009). This suggests that a combination of risk factors is likely to increase the carcinogenic rate.

Due to the smoking prohibition issued worldwide, there is a downtrend in oral cavity cancer incidence within several countries. Conversely, an increasing rate of oropharyngeal and oral cavity cancer is being seen in Denmark, the Netherlands, Norway, Sweden, the United Kingdom, Canada, and the US (Chaturvedi et al., 2013). This change could be attributed to infection with human papillomavirus (HPV). HPV, a double-stranded circular DNA virus, is demonstrated to be a carcinogenic factor in HNCs. There are over 100 serotypes of HPV with different degrees of carcinogenicity, including high-risk HPV16, HPV18, HPV31, HPV33, and HPV 35 (Hennessey, Westra, & Califano, 2009). Currently, HPV infection greatly increases the risk of HNC, being associated with 70% of oropharyngeal cancer in the UK; other tumour sites show low virus load and integration (Koskinen et al., 2003). HPV oncoproteins E6 and E7, expressed continuously within host cells, can promote the development of cancer by inhibiting the function of pRb and p53, the key tumour suppressor genes regulating the progression of cell cycle from G1 to S phase.

HPV is known to be a good prognostic factor for patients with oropharyngeal cancer, but the prognostic value of HPV-positive status to cancers elsewhere in the head and neck is still unknown. A short overview of clinical and biological differences between HPV- positive and -negative HNC is presented in Table 1. Overall, HPV positive HNC patients have a higher two-year overall survival (95%) than patients with HPV negative (62%) (Vokes, Agrawal, & Seiwert, 2015). Up to now, prospective studies have not established concrete therapeutic approaches in HNC based on HPV status (Gillison et al., 2019; Mehanna et al., 2020). There are experimental studies that reveal different effects of drugs in relation to HPV status. HPV-positive HNC cell lines displayed increased sensitivity to a combination of platinum and radiation (Ziemann et al., 2015). Due to the potential effects of HPV infection on drug response, HPV status should be considered when studying potential new drugs for HNC treatment.

Table 1. A short overview of clinical and biological features of HPV-positive and HPV-negative head and neck cancer patients. It was adapted from HPV Positive Head and Neck Cancers: Molecular Pathogenesis and Evolving Treatment Strategies (Dok & Nuyts, 2016).

	HPV-positive	**HPV-negative**
	Clinical and Epidemiological characteristics	
Incidence	Increasing	Decreasing
Age	Younger	Older
Socioeconomic status	Higher	Lower
Risk factors	Sexual behaviour, marijuana exposure	Tobacco and alcohol exposure
Anatomical location	Oropharynx	All head and neck sites
Prognosis	Good	Poor
	Biological and Histopathological characteristics	
TP53 pathway	E6 mediated degradation	TP53 mutations
RB pathway	E7 mediated degradation	Inactivating mutations or other alterations in pathway
p16INK4a expression	Overexpressed	Under-expressed
Histology	Poorly differentiated or basaloid SCC	Modestly to well differentiated, keratinized SCC

2.2.3 Molecular biology of head and neck cancer

HNC development is generally considered a complex and chronic pathological process. It is affected by many factors, such as host molecular genetic factors and environmental factors. Several researchers have proposed a novel model of HNSCC progression, with genetic instability increasing from normal epithelium, to hyperplasia, dysplasia, carcinoma in situ, and finally invasive carcinoma. In this process, multiple genetic or epigenetic alterations occur, including loss of heterozygosity of chromosomes 9p21 (p16-INK4a), 3p21, 17p13,

13p21, 14q24, 4q26-28, 6p and 8p23 and gain of 11q13 (Forastiere et al., 2005; Haddad & Shin, 2008; Leemans, Braakhuis, & Brakenhoff, 2011; Lippman & Hong, 2001). Currently, the known oncogenes involving in HNC include growth factor and receptor, Ras gene family, Myc gene, and apoptotic genes (survivin, Bcl-2, Bcl-1, CCND1). The results of deep sequencing of the whole genome suggest that HNC may be mainly due to the inactivation of tumour suppressor genes. The most frequently changed tumour suppressor genes are p53, Notch1, Rb, p16(CDKN2A), FAT1, PTEN and FAS (Jiang, Ye, Dong, Hu, & Xiao, 2019; Leemans, Snijders, & Brakenhoff, 2018). Of these, p53 is the most commonly mutated gene in HNC, with mutations in 72% of HPV- and 3% of HPV+ HNCs (Leemans et al., 2018; Puram & Rocco, 2015). Overall, it was found that mutations occur mostly in tumour suppressor genes and mutations in oncogenes are uncommon. Unfortunately, mutations in tumour suppressor genes are difficult to target, and the potential for oncogenes to become targets in therapy is very limited (Puram & Rocco, 2015).

With the development of technical approaches for whole genome analysis, a deeper comprehension of genetic changes in HNC has been achieved. The common alterations in genes involved in key signalling pathways (Leemans et al., 2018; Puram & Rocco, 2015) can be summarised as follows: i) p53 related cell cycle control (p53/Rb/p16/CCND1) (proliferation and apoptosis). ii) EGFR-RAS/MAPK/PI3K/PTEN (cell survival). iii) WNT signalling pathway and NOTCH1 and FAT1 (cell adhesion and orientation). iv) TGFβR/SMAD signalling and K-Ras (cell adhesion and invasion). My project will follow the genetic changes and molecular pathway with perphenazine related literature review to understand the background of the potential relationship between perphenazine and head and neck cancer.

In addition, studies of epigenetic modifications such as DNA methylation and histone methylation or acetylation which regulate gene expression are important for improving the clinical diagnosis and treatment of HNC. Investigators tested p16, MGMT, GSTP1, and DAP kinase in serum samples from 95 patients with head and neck primary tumours. They found

that 52 of the samples had hypermethylation of at least one gene, and 21 samples showed consistent types of methylation. Promoter methylation may provide an effective serum test for monitoring HNC patients (Sanchez-Cespedes et al., 2000). Since epigenetic modifications and regulation are reversible kinetic processes, therapeutic modalities targeting epigenetics offer an optimistic outlook for HNC. Reversal of DNA hypermethylation and histone deacetylation may result inhibition of tumour growth and/or invasion. The relevant drugs can be classified into two groups: DNA methyltransferase inhibitors (DNMTi) and histone deacetylase inhibitors (HDACi). The use of these epigenetic drugs in HNSCC can block tumour growth like Zebularine (DNMTi), restore sensitivity and reduce cytotoxic dose in cisplatin treatment like decitabine (DNMTi) and improve the efficacy of cisplatin like MS275 (HDACi) *in vitro* and *in vivo* (Castilho, Squarize, & Almeida, 2017; Gasche & Goel, 2012; Rikiishi et al., 2007; Suzuki, Shinohara, Nishimura, Echigo, & Rikiishi, 2007).

2.3 Current trend in Cancer drug discovery

Based on a deeper exploration of the hallmarks of cancer and its specific genetic changes, therapeutic targets can be found and translated into drug discovery for improving cancer treatment (Figure 2), for example EGFR and PD-1 inhibitors in HNC

Currently, there are 130 to 150 approved cancer drugs routinely being applied for cancer treatment. Some of them were not originally designed for treating cancer. Fifty-seven new oncology drugs have been launched in the past five years (*IQVIA Global Oncology Trends*, 2019), and this number will continue to rise steadily in the future. With the increasing investment in the drug discovery market, the research and development costs are increasing year by year. However, there are problems in new drug discovery. It is a lengthy process – the new oncology drug approval process usually takes about 14 years (median time; IQVIA Global Oncology Trends 2018). Furthermore, not all of the novel oncology drugs can be registered successfully by the Food and Drug Administration (FDA). About 99.9% of novel agents fail early phase screening or validation in the traditional drug discovery process (Sleire et al., 2017). Only 5% of novel drugs in Phase I clinical trials secure FDA approval (Gupta,

Sung, Prasad, Webb, & Aggarwal, 2013). All these factors make the price of the available new oncology drug exorbitant. Therefore, facing the expensive cost and low success rate, scientific research attempts to find cheaper and more rapid methods to achieve a better outcome.

So far, many efforts have been made to accelerate the time and decrease the cost so as to bring a new cancer medicine to patients as soon as possible. One method is to repurpose an existing FDA approved drug (see section 1.4). My project aims to repurpose one of the antipsychotic drugs, perphenazine, for treating HNC.

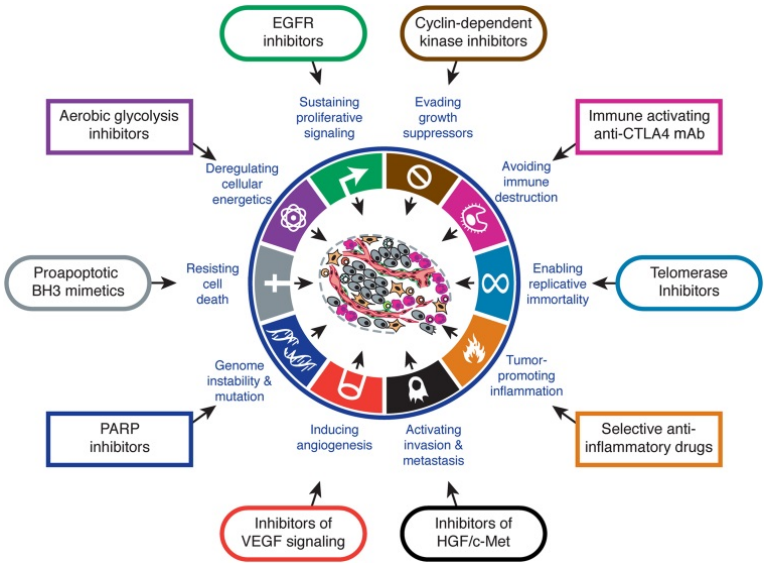


Figure 2. Therapeutic Targeting of the Hallmarks of Cancer (Hanahan & Weinberg, 2011). Drugs that interfere with each of the targets associated with cancer development. Each of them belongs to the enabling characteristics and emerging hallmarks displayed in Figure 2.

2.4 Cancer Drug Repurposing

The term 'drug repurposing' refers to the use of FDA or EMA approved drugs for another indication, rather than their initially approved use. Repurposing existing drugs for cancer therapy can be valuable since safety profiles are known, leading to higher success rates and reduced development times. It subsequently leads to lower costs compared with the traditional development of novel therapeutics. The time taken to gain clinical approval for repurposed drugs is usually considerably shorter than the 10-17 years for novel therapeutics

with estimations around the 3-12 years (Ashburn & Thor, 2004). Success rates for market approval approach nearly 30% compared to only around 10% for new drugs (Kaiser, 2011).

As mentioned in section 1.3, not all anti-cancer drugs were originally designed for treating cancer. Some of them have been repurposed, and they can be classified in a way that aligns with the hallmarks of cancer (Figure 2). Some potential approved drugs will be discussed as they offer an insight. The first one is metformin, which is the first-line drug for treating type II diabetes. With the development of epidemiology and the application of biostatistics, diabetic patients treated with metformin were found to have a lower incidence of cancer development and decreased mortality compared with other diabetic patients not taking metformin (Sleire et al., 2017). According to Sleire et al. (2017), the anti-cancer mechanism of metformin is associated with several hallmarks of cancer, such as resisting programmed cell death, deregulating cellular metabolism, and sustaining proliferative signalling. Metformin has been shown to inhibit glycolysis (Pollak, 2014) and induce apoptosis by causing ER Stress (Yang et al., 2015). It can also activate AMPK to inhibit anabolic pathways (Anand et al., 2008; Hardie, 2003; Horman et al., 2002) and inhibit mTOR, reducing cell growth.

Some antipsychotic drugs have also been indicated as potential anti-cancer drugs, because they may inhibit cancer growth in melanoma, leukemia, or other cancers (Gil-Ad et al., 2006; Zhelev et al., 2004). Phenothiazines are widely used as antipsychotics. They mainly act on dopamine receptors in the central nervous system. Most have sedative, antiemetic, antipsychotic, and hypothermia effects. Because phenothiazines have different degrees of antiemetic, sedative, and analgesic effects, they were combined with chemotherapy drugs to reduce the side effects induced by chemotherapy. The representative drug of phenothiazines is chlorpromazine. With the increasing clinical application, more and more research found that chlorpromazine may inhibit cancer proliferation and facilitate apoptotic activity. It can induce cell cycle arrest by increasing the expression of p21, which usually is mediated by p53 (Shin et al., 2010), and increase p53 associated apoptotic activity (Lee et al., 2015). A study

also indicated that chlorpromazine could down-regulate the Akt/mTOR signalling pathway involved in autophagy (Shin et al., 2013). In addition to apoptosis and autophagy, cancer angiogenesis and invasion may be affected by chlorpromazine treatment by interfering with β-catenin signalling (Pulkoski-Gross et al., 2015). Apart from chlorpromazine, two more antipsychotic drugs, penfluridol, and fluspirilene, also show similar anti-tumour potential.

In summary, there is increasing public attention on the cancer drug repurposing market; some of the current drugs, such as thalidomide and raloxifene, have been marketed and used in cancer treatment (Sleire et al., 2017). In my project, I will focus on perphenazine (PPZ) and its potential repurposing for HNC treatment. As a member of the phenothiazines, perphenazine shares a similar chemical structure with chlorpromazine which has anti-cancer function. We hypothesize that PPZ may show an anti-cancer effect as an anti-tumour agent in head and neck cancer.

2.5 Perphenazine

Perphenazine (PPZ), a member of the phenothiazines group, is the first-generation antipsychotic drug developed in the 1950s. It can bind the dopamine D2/D1 receptor as a dopamine antagonist to treat psychotic disorders, such as schizophrenia. It can also inhibit calmodulin, hence modulating a series of cell activities such as apoptosis and metabolism. As a medium-potency antipsychotic drug, PPZ is not widely used now due to the development of new drugs with a more favourable side effect profile. The toxicity of perphenazine is low, but its antipsychotic effect and particularly its antiemetic effect are strong. The sedative effect of perphenazine is weak, which is desirable, and it is effective for hallucinations, delusions, anxiety, nervousness and agitation. Therefore, it can be used to treat positive symptoms of psychosis, but for negative symptoms of schizophrenia, its effect is unclear (King, 1998). Extrapyramidal side effect of PPZ are often seen, such as acute dyskinesias, dystonic reactions, and akinesia but also akathisia (more common with high doses of perphenazine).

The oral bioavailability of PPZ is approximately 40%, and it has a half-life of 8 to 12 hours (up to 20 hours). Two or three divided doses usually will be given in each day for patients who have a psychotic disorder. Because of its sedation and hypotension effect, it is possible to provide two-thirds of the daily dose at bedtime and one-third during breakfast to achieve its hypnotic activity during the night and to keep normal daytime vitality without loss of therapeutic activity.

2.5.1 Perphenazine in cancer

In addition to antipsychotic medication, PPZ has been identified as a potential cancer treatment drug with its anticancer effect mediated via protein phosphatase 2A (PP2A) activation in leukaemia cells (Gutierrez et al., 2014). Since the targets of PP2A are associated with oncogenic signalling cascades, such as Akt, Myc, ERK, MEK and Raf, PP2A is more likely to function as a tumour suppressor via de-phosphorylate of key substrates.

Gutierrez et al. (2014) proposed a mechanism-of-cation for PPZ form analysis in T cell acute lymphoblastic leukaemia (T-ALL), which provides some clues for my further study in HNC. They noted that PPZ not only inhibits leukaemia cell viability, but also can induce its apoptosis. In their study, both NOTCH (often mutated in HNC; (Leemans et al., 2018)) dependent and independent T-ALL cell lines were treated with gamma-secretase inhibitor (GSI; to block NOTCH1 generated ICN1 from targeting Myc), or PPZ, or the combination. PPZ alone inhibited cell viability in all selected cell lines tested and an enhanced effect with the combination treatment of PPZ and GSI was found. These results indicated that PPZ activity is independent of NOTCH mutation in T-ALL cell lines. A PPZ concentration-dependent increase in caspase3/7 in T-ALL provided evidence of PPZ's ability to induce apoptosis, and its apoptotic effect could also be enhanced when combined with GSI treatment. Further investigation revealed that PPZ activity could be blocked by BCL2 overexpression, suggesting that PPZ induced apoptosis is mediated through a mitochondrial pathway.

Gutierrez et al. (2014) thought there was no relationship between dopaminergic signalling and anti-leukemic activity of PPZ and related phenothiazines, even though dopamine receptors are associated with immune regulation. This conclusion was based on testing the drug promethazine, a member of the phenothiazines. Promethazine has an anti-leukemic effect in both human T-All cell lines and a zebrafish model, but it is not a dopamine inhibitor. The calmodulin pathway of anti-cancer activity was also abrogated in this study via a selective calmodulin inhibitor, W13, but this was highly toxic to zebrafish larvae at a low nanomolar concentration.

This was the first study to identify PP2A as a target of PPZ activity in cancer; in vitro and in vivo experiments showed that PPZ can target PP2A to de-phosphorylate downstream substrates - such as Akt (cell survival), ERK (ERK activation), p70S6K - thus blunting their activity. The pro-apoptotic protein BAD can also be de-phosphorylated by PPZ enabling it to induce cell death. Furthermore, PPZ can down-regulate Myc expression, thereby inhibiting cell growth. To summarise, Gutierrez et al (2014) think PPZ can target PP2A to induce mitochondrial apoptosis and inhibit T-ALL growth by de-phosphorylation of multiple PP2A substrates.

At present, there are limited published articles on the relationship between cancer and PPZ. I have been unable to find any published articles relevant to HNC. Therefore, the detailed mechanism still needs further exploration.

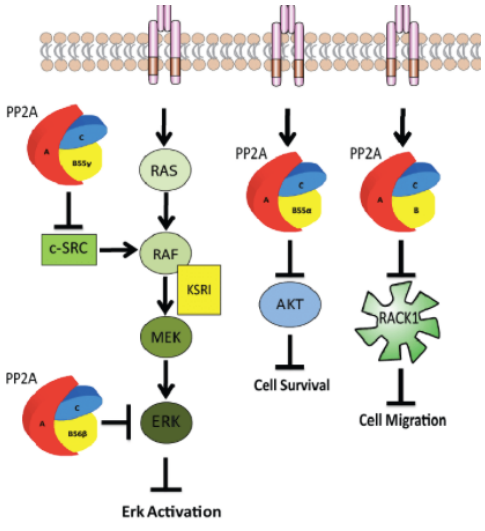


Figure 3: PP2A as a tumour suppressor in signalling pathways (Kiely & Kiely, 2015). The MAP kinase pathway can be negatively regulated by the PP2A holoenzyme via inhibition of c-SRC. ERK activation can also be inhibited via direct dephosphorylation by PP2A. PP2A can negatively regulate AKT activity and hence cell survival. Cell migration can also be indirectly affected by PP2A.

2.6 AcceleraTED (in InHANSE)

The Institute of Head and Neck Studies and Education (InHANSE) - whose research focuses on diseases of the head, neck and thyroid - has established and validated a multi-disciplinary, multistage, integrated drug repurposing platform. It is called the "Accelerated Translation of therapeutic agents and Emerging Devices in Head and Neck and Thyroid cancer" (AcceleraTED) platform. This platform is mainly based on repurposing non-oncology FDA-EMA approved drugs for the new treatment of HNCs. Combined cisplatin chemotherapy and radiation is currently the most effective treatment for HNC patients with locally advanced, unresectable tumours (Brana & Siu, 2012). However, these treatments have severe side-effects, such as hair loss, strong gastrointestinal reactions, and generalised weakness. Therefore, the AcceleraTED platform aims to find alternative drugs that may replace or reduce the amount of cisplatin required. There are five main stages to this platform.

Stage I is the primary screening of drug libraries using high throughput viability screens to identify drugs that reduce viability of HNC cell lines by $\geqslant 50\%$. The two main libraries used by the InHANSE group are (i) the FMC repurposed drugs library provided by Dr Khanim, Prof. Drayson and Prof. Bunce; University of Birmingham; and (ii) the commercially available Prestwick library (Bryant et al., 2019). These are comprised of generic British National Formulary/FDA/EMA approved drugs identified via literature review to show potential anti-cancer activity.

Stage II is the secondary screening, validating findings from stage I by a series of experiments including: concentration-response using the AlamarBlue Assay, clonogenic survival, and

induction of cell death via apoptosis (Annexin V) or autophagy. These experiments are conducted using a panel of HNC cell lines.

Stage III is a confirmation stage, assessing activity against primary cancer cell cultures collected through our optimised tissue sample collection platform (appropriate ethical approval is in place). The primary cell samples are donated by HNC patients treated at the Queen Elizabeth Hospital, Birmingham.

Stage IV is tertiary screening, using animal models to provide a better understanding of the efficacy and toxicity of the selected agent. Mouse xenograft models are used for this stage.

The final stage is to take the most successful drugs from stages 1 to 4 into human trials to test the safety of agents in combination with standard-of-care, with the hope of providing novel treatments (Bryant et al 2019).

2.7 Current Project outline

Initial screening of the Prestwick Chemical Library using a high throughput AlamarBlue cell viability screen identified PPZ as a potential hit (Figure 4) by previous investigators from InHANSE group.

My research utilised the AcceleraTED platform to further investigate PPZ as a potential re-purposed agent for HNC treatment.

In my project, I have undertaken the secondary (*in vitro*) screening to assess the PPZ concentration response in the FaDu and Cal27 cell lines, in the presence or absence of cisplatin (standard-of-care treatment for HNC). Further, I have evaluated the colony-forming ability by clonogenic assay in both FaDu and Cal27 cell lines. The cell death assessment experiments measured (i) apoptosis via Annexin V/propidium iodide staining and flow cytometry and (ii) autophagy via expression of the surrogate marker LC-3 by Western Blot in FaDu cell lines. For the Cal27 cell line, only apoptosis ability was assessed, and its relationship between autophagy and PPZ needs further study. I wanted first to investigate the more severe case scenario since HPV negative patients tend to have worst treatment response. Future experiments should evaluate HPV-positive cell lines too. However, course deadline

and Covid-19 constrain as well as budget did not allow me to check completion for this project. In addition to the core work of the AcceleraTED platform, a series of experiments exploring the mechanism of action of perphenazine in HNC were also pursued.

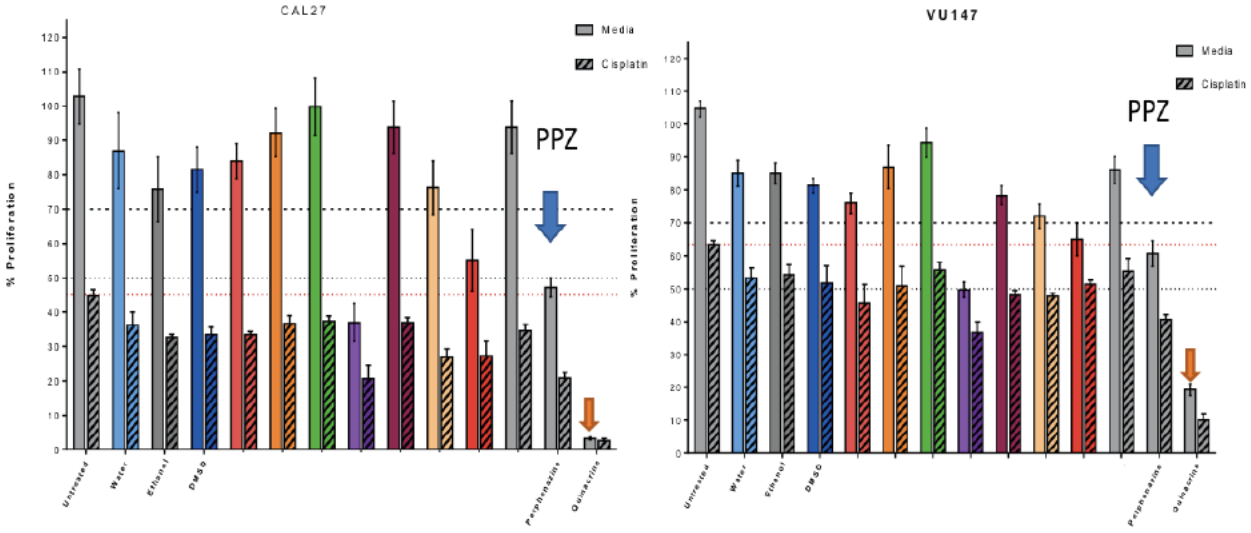


Figure 4: Initial screening of drugs in the Prestwick Chemical Library ® ± cisplatin.
Cell lines treated with 10μM PPZ +/- 2μM cisplatin (Blue arrows) showed the second-lowest levels of proliferation. Quinacrine (orange arrow) has been assessed previously and this study is published (Bryant et al., 2019).

2.8 Aims and Hypothesis

The broad aim of my MRes. thesis was to investigate the anti-cancer effects of PPZ *in vitro*.

The specific aims were:

1. To determine the effects of PPZ +/- cisplatin on HNC cell line viability and proliferation, clonogenic survival, apoptotic cell death, using the AcceleraTED platform.

2. To identify potential mechanism(s) through which PPZ mediates its effects.

Hypothesis: PPZ inhibits the proliferation and clonogenic survival of HNC cell lines and/or induces apoptosis via the activation of PP2A

3. Methods and Materials

3.1 Cell lines and Reagents

Commercially available HNC cell lines were used to assess the effects of PPZ. FaDu (HTB-43; ATCC) and Cal27 (ACC-446; DSMZ) cells were utilised in this project, and the detailed information is shown in Table 2. Dulbecco's Modified Eagle's Medium (DMEM) high glucose supplemented with 10% Foetal bovine serum, 1% Penicillin Streptomycin, 1% L-glutamate, and 1% Non-essential amino acids were used for both FaDu and Cal27 cell culture. Cells were cultured in high humidity Panasonic incubators at 37°C with 5% CO2. Regular mycoplasma screening was performed to prevent cell infections and annual genetic verification undertaken using Short Tandem Repeat (STR) profiling to confirm identity.

Table 2. FaDu and Cal27 cell line features. Mutation data are available from the Catalogue of Somatic Mutations in Cancer (https://cancer.sanger.ac.uk/cosmic).

	FaDu	***Cal27***
Cell type	Hypopharyngeal squamous cell carcinoma	Tongue squamous cell carcinoma
Species	Homo sapiens	Homo sapiens
Growth properties	Adherent	Adherent
HPV status	Negative	Negative
Mutations	CDKN2A homozygous SMAD4 homozygous TP53heterozygous TP53 heterozygous	CDKN2A homozygous SMAD4 homozygous NRAS unknown TP53 homozygous

All reagents for cell culture were purchased from Sigma-Aldrich®, and cell culture vessels from Corning®, unless stated otherwise. Cells were trypsinised, counted, and diluted to an appropriate density as follows. Firstly, cell cultures were gently washed using sterile

phosphate buffered saline (PBS) and then incubated in 1x Tryp1E (12605-010; Gibco®) to detach cells. After centrifugation, the supernatant was discarded, and cell pellets were re-suspended in an appropriate volume of fresh media. 10µl of cell suspension was then gently mixed with an equal volume of 0.4%Trypan Blue (T10262; ThermoFisher) for counting using a Cell Countess TM Automated cell counter (Invitrogen).

Perphenazine (Sigma Aldrich®) was dissolved in 100% ethanol as a vehicle, preparing 99 mM stock. The prepared stock was frozen at -20°C for use in experiments as required. 3mg Cisplatin (BioVision) was dissolved in 1ml dimethyl sulfoxide (DMSO) (Sigma Aldrich®), and then it was stored at -20°C and utilised within seven days.

3.2 AlamarBlue viability Assay

AlamarBlue viability Assay is a rapid and sensitive assay for cell proliferation and cytotoxicity by measuring cell viability. AlamarBlue (Invitrogen), is an immediate and non-toxic blue redox indicator. Its active ingredient resazurin is phagocytosed by living cells; metabolic reduction then produces resorufin, which is pink and highly fluorescent. To determine the effect of PPZ on cell viability and to see if this effect is concentration-dependent, we used PPZ in the range of 3µM to 30µM ± 2µM cisplatin in both Cal27 and FaDu cell lines. In addition, cisplatin concentration response experiments, in the range of 0.01µM to 10000µM, with perphenazine at 3µM, 6µM, and 10µM were undertaken using AlamarBlue viability assays.

3.2.1 Perphenazine concentration-response ± 2 µM cisplatin

FaDu and Cal27 cells were seeded at 4000 cells per well into 96-well plates in 100µl of media. After 24h incubation, cells were treated with increasing concentrations of PPZ (3µM, 5µM, 10µM, 12µM, 15µM, 17µM, 20µM, 30µM) with either 2µM cisplatin or media. Concentrations stated are the final values in a total volume of 200µl per well. Additional control wells included media only (no cells), no drug (cells + media) and vehicle control (cells + ethanol or DMSO for PPZ and cisplatin respectively).

All the plates were treated with the drug for 72 hours. 68 hours after the addition of drugs, 20µL AlamarBlue ® reagent (DAL1100; ThermoFisher) was added to each well. 4 hours after the addition of AlamarBlue, plates were read using a PHERAstar ® FS plate reader at 540/590nm.

3.2.2 Cisplatin concentration response with perphenazine

Similar to the PPZ concentration response ± 2µM cisplatin, suspensions with 4000 cells from FaDu and Cal27 cell lines were seeded into the experimental plate. The media plate with no cells was used as a negative control group for assay interference assessment. Untreated control, vehicle control, and media + perphenazine wells were included on each plate. Increasing concentrations of cisplatin (0.01µM, 0.03µM, 0.1µM, 0.3µM, 1µM, 3µM, 10µM, 30µM, 100µM, 300µM, 1000µM) were added to planned wells for drug treatment with three different concentrations of PPZ (3µM, 6µM, and 10µM). AlamarBlue was added after 68 hours and plates were read by PHERAstar ® FS plate reader, as above.

All treatments were conducted in triplicate for both the perphenazine and cisplatin concentration-response assays. The mean of the three absorbance values was calculated and normalised to the corresponding control plate, and values generated as % of untreated. Four parameter logistic regression models were used on GraphPad Prism 7.0 software for data analysis and for generating related concentration-response curves. The IC_{50} at 72h treatment was calculated and is shown in Figures 5 and 6.

3.3 Clonogenic Cell Survival Assay

Clonogenic cell survival assays are an effective method to determine the colony-forming ability as a measure of proliferation, in the presence and absence of drug treatment (Franken et al., 2006). FaDu and Cal27 cells were treated with increasing concentrations of perphenazine (3.5µM, 5.1µM, 6.7µM, and 12.9µM) with or without 1.25µM cisplatin and 0.5 Gray irradiation (IR) treatment.

Cal27 and FaDu cells were seeded at 1250 cells/ml into 10cm plates (8ml/plate). After 24h incubation at 36.5°C, 5%CO_2, 50% of the media was removed from all dishes, leaving cells in 4 mL of media in each plate. Dishes were sealed with parafilm and irradiated prior to additional drug treatment. Four dishes comprised the control group: untreated (negative control) cisplatin only, irradiation only, and cisplatin plus irradiation. The treatment group, as mentioned above, contained four perphenazine-only groups and four perphenazine with cis + IR groups. After 24hours treatment, media was removed and replaced with fresh media (no drug treatment). Plates were then left in the incubator for 12 to 14 days (until colonies were detectable, but not excessively merged). Subsequently, the clonogenic assay plates were washed gently with PBS and distilled water, followed by a staining step with Crystal Violet (0.5% w/v) staining, containing glutaldehyde (6% v/v) for 30 minutes and finally they were left to air dry.

All dishes were digitally scanned, and the number of colonies was counted using ImageJ colony counting plugin software, and then, their plating efficiency (PE) and survival factor (SF) were calculated as a % of untreated using Excel. At least four independent experiments were analysed in a two-way ANOVA with Dunnett's multiple comparison test using GraphPad Prism 7.0.

3.4 Apoptosis assay assessed by Annexin V

Annexin V staining, paired with propidium iodide (PI), is widely used to identify the stages of apoptosis and/or another cell death by flow cytometry analysis. Annexin V positive staining identifies apoptotic cells, and annexin V/ PI co-positivity indicates later stages of apoptosis. PI staining without annexin V staining is an indicator of other modes of cell death, such as necrosis. The apoptotic effect of PPZ was assessed at different concentrations (3.5μM, 5.1μM, 6.7μM, and 12.9μM) with or without 2μM cisplatin using FaDu and Cal27 cells.

8.0x 10 FaDu cells or Cal27 cells per well were seeded in 6-well culture plates (COSTAR) for 24 hours incubation at 36.5°C, 5%CO_2. Cells were then exposed to increasing concentrations of perphenazine (FaDu: 3.5μM, 5.1μM, 6.7μM, and 12.9μM; Cal27: 3.5μM,

10μM, 12.9μM, and 14.5μM) with and without 2μM cisplatin. The control group included five different controls: negative control-untreated, 0.04% vehicle control-ethanol or DMSO; positive control- 2 and 10μM cisplatin. After 48-hours of treatment, cells were harvested and stained via the following steps: removing media, detaching cells, and then transferring cells into FACs tubes. Next, all tubes were centrifuged at 1100 rpm for 4minutes (Allegra ® X-12R Centrifuge, Beckman Coulter), washed in cold PBS and re-centrifuged. In the staining step, 200μl PBS was added to the unstained control, 100μl of Annexin-binding buffer (ABB) (1x) with 5μl Alexa flour 488 Annexin V and 100μl ABB (1x) with 1μl PI were added to 10μM cisplatin treated cells with Alexa flour 488 Annexin V staining. Also10μM cisplatin treated cells were incubated with PI staining controls respectively for allowing compensation for fluorochromes. 106μl of master mix (100μl 1x ABB, 5μl Alexa flour 488 Annexin V and 1μl 100ug/ml PI) were prepared and added into cell pellets in all other tubes. All samples with appropriate stain were incubated at room temperature for 15 minutes. Cal27 cells were fixed by 1% formaldehyde solution (Thermo scientific®) for 10 minutes and then washed prior to analysis.

After the appropriate set up of compensation controls, 10000 to 50000 cell events in each sample were collected and recorded using a Flow cytometer (BD LSR-II) and BD FACSDIVA™ software. All data were analysed using the Kaluza Analysis v.2.1.1 software (Beckman Coulter). Statistical analysis was undertaken by using a two-way ANOVA with Dunnett's multiple comparison test in GraphPad Prism 7.0.

3.5 Cell cycle assay

Sample preparation for the cell cycle assay used the same procedure as Annexin V assay before PI staining. The prepared cell cycle buffer (10ug/ml PI, 0.1M sodium chloride and 1% triton x-100 in distilled water) was added to each sample; samples were then incubated in the dark at 4°C for 1 hour. Data was collected by flow cytometry, recording 20,000 events, and then analysed using the Kaluza Analysis v.2.1.1 software (Beckman Coulter) and a two-way ANOVA with Dunnett's multiple comparison test in GraphPad Prism 7.0

3.6 Protein Quantification and Expression by Western Blot

Western blot analysis was used to determine the difference in expression levels of certain proteins after PPZ treatment of FaDu cells in order to investigate the mechanism of action of perphenazine.

FaDu cells were seeded at 2 x 10^6 cells/10cm culture dish, 6ml media were then added to each dish. After 24h, appropriate drugs or ethanol were added for treatment. Dishes were treated with different PPZ concentrations (5μM, 7μM, 10μM), or 2μM of cisplatin, or a combination of 7μM perphenazine and 2μM of cisplatin; two negative controls (untreated (media) and vehicle (ethanol) were also set up.

After 24h treatment, cells were collected from each plate and washed twice with cold PBS. Samples were then treated by adding 100μl prepared Lysis buffer (RIPA buffer, phosphatase inhibitor, protease inhibitor, and ethylenediaminetetraacetic acid (EDTA)) (ThermoFisher Scientific), followed by incubating them on ice for 5 minutes. All samples were then centrifuged at 14,000xg for 5 minutes to pellet cell debris. The supernatant was transferred into a new 0.5ml Eppendorf tube and stored at - 20°C for protein quantification and SDS-PAGE.

Protein was quantified using the Pierce™ BCA protein assay kit (23227; ThermoFisher) according to the manufacturer's instructions. In the first step bovine serum albumin (BSA) (ThermoFisher Scientific) was prepared and diluted in RIPA buffer to concentrations between 25 and 2000μg/ml for use as standards. 10 μl of each test protein sample and 10 μl of related BSA standard (low concentration to high concentration) were added to duplicate wells in a 96-well plate, followed by adding 200μl of the BCA working reagent (50 (Reagent A): 1 (Reagent B)). Plates were covered with film and incubated at 37°C for 30 minutes. Absorbance was then measured at or near 562nm using a PHERAstar® FS plate reader at room temperature. Blank corrected BSA values were used to plot a standard curve from which the concentration of test protein samples was calculated.

Next, the volume of each sample required was calculated based on the quantification results from BCA assay, and mixed with Laemmli sample buffer (50µL ß-mercaptoethanol (Sigma Aldrich ®) to every 950µL 4× Laemmli buffer (Bio- Rad Laboratories inc.) at a 3:1 ratio. Samples were incubated at 95°C for 5 minutes, then on ice for 5 minutes to ensure complete denaturation, and then they were centrifuged. Mini-PROTEAN Tetra Cell (4 - 20% gradient, 15wells) pre-cast gels (Bio-Rad Laboratories inc.) were prepared for running, and each sample – plus the molecular weight ladder - added as planned to the wells. The whole electrophoresis tank was filled with Tris-Glycine-SDS (TGS) buffer the gel was run at 100V until the dye front reached the line indicator in the tank; the gels were then gently removed, and transferred onto the prepared membranes (Bio-Rad Laboratories inc.) using Trans-Blot ® Turbo TM (Bio-Rad Laboratories inc.) in 15 minutes.

Membranes were blocked with 5% semi-skimmed milk powder (Sigma Aldrich ®) in Tris-buffered saline (Bio-Rad Laboratories inc.) and 0.1% Tween (Sigma Aldrich ®) (TBS-T). The primary antibodies were diluted to the optimised concentration (see Table3) in 5% BSA in TBS-T. They were added in an appropriate volume to ensure the surface of the membranes was completely covered and incubated on a shaker overnight at 4°C. The membrane was then washed three times with TBS-T before adding the secondary antibody, diluted 1:1000 (1g/L anti-rabbit (Promega) or 1g/L anti-mouse (Dako, Denmark)) and 0.2µL precision protein strep actin-HRP conjugate (Bio-Rad Laboratories inc.). After 1 hour of incubation with secondary antibody, the membrane was washed in TBS-T and TBS to clean the membrane surface, then incubated for one-minute with the enhanced Chemiluminecent (ECL) reagent (Bio-Rad Laboratories inc.). In the end, the expression of each protein on the membranes was visualised using a ChemiDoc TM XRS+ and Image LabTM software.

Table 3: Antibody information used in Western Blotting

Name	MW (kDa)	Company	Cat No.	Dilution	Secondary
p21	21-25	SantaCruz	sc-53870	1 in 1000	Mouse
LC-3 (I&II)	19 (I), 17 (II)	NovusBio	NB100-2220	1 in 1000	Rabbit
p53	53	SantaCruz	sc-126	1 in 1000	Mouse
beta-actin	45	Cell Signaling	#4970	1 in 1000	Rabbit
AKT	60	Cell Signaling	#9272	1 in 1000	Rabbit
pAKT	60	Cell Signaling	#4060	1 in 1000	Rabbit

3.7 Statistical Analysis

All results are summarized from more than four independent experiments (unless otherwise stated). Responses to treatments are represented by the mean ±SEM or SD, as indicated. Statistical analysis and comparison of results used one- or two-way ANOVA (Dunnett's multiple comparison test) performed using GraphPad Prism 7 (GraphPad Software, La Jolla, CA, USA). Statistical significance is determined by $p<0.05$.

4. Results

4.1 Perphenazine decreases viability of HNC cell lines

4.1.1 Perphenazine concentration-response with ± 2 μM Cisplatin

To determine whether cell viability will be decreased by PPZ in a concentration-dependent manner, both HNSCC cell lines CAL27 and FaDu were treated with eight different concentrations (between 1-30µM) of PPZ used for the AlamarBlue viability assay with or without standard-of-care cisplatin at 2µM.

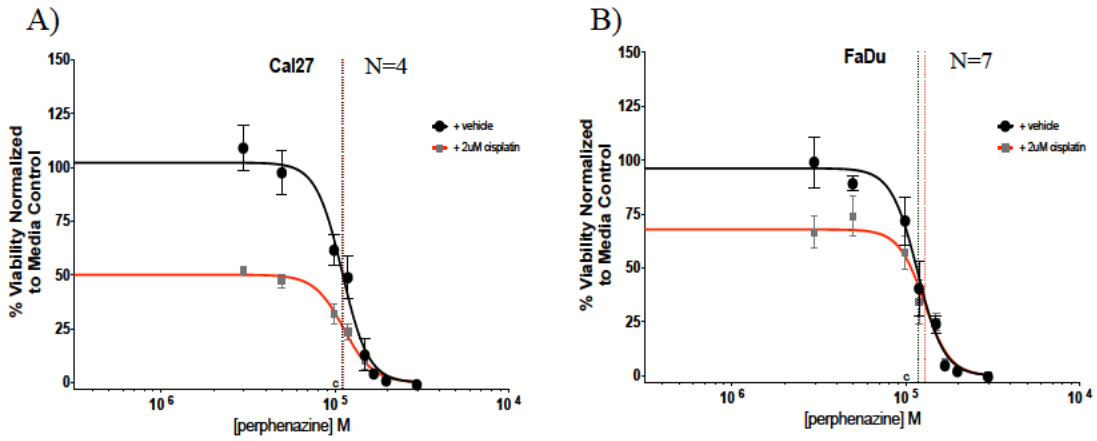


Figure5. PPZ concentration-response curves for Cal27 (A) and FaDu (B) cell lines (N≥4). Cells were treated with PPZ at the specified concentrations for 72 hours, with (red curve) or without (black curve) 2µM cisplatin and viability assessed by AlamarBlue assay. Data are shown as the mean ±SEM. Vertical lines highlight IC_{50} values, colour matched.

A reduction in cell viability was demonstrated at higher concentrations (5µM to 30µM) of PPZ, with IC_{50} values of 11.0 and 11.9µM for the PPZ only group, in Cal27 and FaDu respectively (Figure 5A and 5B: black line), indicating a similar sensitivity to PPZ for both HNSCC cell lines. IC_{50} value refers to the concentration of PPZ that gave a 50% reduction in cell viability relative to its maximum effect.

As the standard-of-care chemotherapy treatment in HNC, cisplatin was also evaluated with PPZ to detect whether PPZ efficacy can be affected by cisplatin. For concentrations of PPZ exceeding 5µM, the PPZ and PPZ plus cisplatin curves illustrated a reduction of cell viability for both cell lines. Addition of 2µM Cisplatin did not improve the inhibitory effect of PPZ on

FaDu cell lines. There was an additional reduction of Cal27 cell viability for PPZ (from 5 to 15μM) with 2μM cisplatin, compared to PPZ alone. However, the IC_{50} values were almost unaffected: 11.0μM for the PPZ only group and 11.3μM for PPZ with cisplatin group (Figure 5A and Table 4). The results of PPZ concentration-response for both HNSCC cell lines, suggest that there is no synergistic effect between PPZ and 2μM cisplatin, especially in Figure 5B. The addition of 2μM cisplatin did not alter PPZ's efficacy against these HNC cell lines.

Table 4: Summary of mean pIC_{50}(M), SEM and IC_{50} (μM) values from PPZ concentration-response curves with or without 2μM cisplatin for Cal27 and FaDu cell lines (N≥4). Response fitted to a four-parameter logistic equation using GraphPad prism 7.

	PPZ only			PPZ+2μM Cis		
Cell lines	pIC50(M)	SEM	IC50(μM)	pIC50(M)	SEM	IC50(μM)
FaDu	4.92	0.02	11.9	4.89	0.03	12.7
Cal27	4.96	0.02	11.0	4.95	0.02	11.3

4.1.2 Cisplatin concentration-response with different Perphenazine concentrations

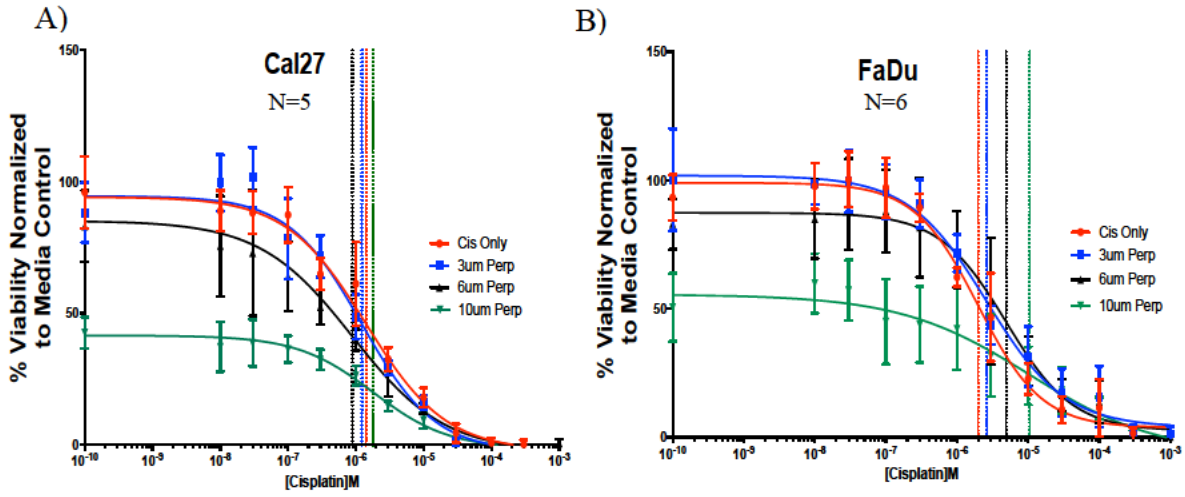


Figure 6: Cisplatin concentration-response + 0, 3, 6, 10μM Perphenazine (72hours) in Cal27(A) and FaDu(B) cell line (N≥5). Cisplatin concentration-response with 0 (red line), 3 (blue line), 6 (black line), 10 (green line) μM Perphenazine for Cal27 (A) and FaDu (B) cell lines. Data are presented as mean ± SD. Vertical lines highlight IC50 value, colour matched.

A PPZ concentration dependent response with 2μM cisplatin was demonstrated for both HNSCC cell lines. To evaluate the effect of cisplatin concentration-response with PPZ treatment, 11 different concentrations of cisplatin ranging from 0.01 to 1000μM alone, or with 3, 6, 10μM PPZ, were added to both Cal27 and FaDu cell lines. At the lower concentration of cisplatin (<0.3μM), there is no difference between cisplatin group and with the addition of 3μM PPZ group (Figure 6). The cell viability of 83.06±13.69% on Cal27 and 82.94±9.80% on FaDu were illustrated on both 6μM PPZ group (black lines) at the lowest concentration of cisplatin, showing a suppression trend of cell viability. The cells treated with 10μM PPZ presented 42.5±5.96% and 50.6±13.20% cell viability, respectively on Cal27 and FaDu cell lines, demonstrating the inhibitory effect of PPZ on HNC cells. This result was similar to previous data presented in Figure 4 (Chapter 1.7) and Figure 5 (IC_{50}:11μM on Cal27 and 11.9μM on FaDu), which showed ~50% cell viability following treatment with 10-11μM PPZ. All the data described above confirm the cytotoxic effect of PPZ on HNC cell lines.

There is decreasing cell viability with increasing concentrations of cisplatin, showing a concentration-dependent effect in the presence or absence of PPZ (0 to 10μM) (Figure 6A

and 6B). The addition of PPZ enhanced the inhibitory effect of cisplatin on cell viability for both HNSCC cell lines, especially the group treated with 10μM PPZ. The IC_{50} values for the Cal27 cell line are 1.42μM for cisplatin alone, 1.23μM for 3μM PPZ, 0.89μM for 6μM PPZ and 1.79μM for 10μM PPZ. For the FaDu cell line, combination of cisplatin with increasing concentrations of PPZ showed increasing IC_{50} values of 1.98, 2.62, 4.91, 10.5μM; however, no significant difference was observed between pIC_{50} values. In terms of the concentration-response curves illustrated for Cal27 and FaDu cell lines, no obvious additive effect was identified; further experiments are needed to confirm this observation.

Table 5: Summary of pIC50(M), IC50(µM), and SEM values of Cisplatin concentration-response ± 3, 6, 10μM perphenazine in Cal27 and FaDu cell lines (N≥5). Response fitted to a four-parameter logistic equation calculated by GraphPad prism 7.

	Cal27			FaDu		
Treatment	pIC50(M)	SEM	IC50(µM)	pIC50(M)	SEM	IC50(µM)
Cis	5.85	0.07	1.42	5.70	0.06	1.98
Cis+3µM PPZ	5.91	0.08	1.23	5.58	0.08	2.62
Cis+6µM PPZ	6.05	0.09	0.89	5.31	0.1	4.91
Cis+10µM PPZ	5.75	0.09	1.79	4.98	0.37	10.5

4.2 Perphenazine reduces colony-forming ability of HNC cell lines

To obtain a better understanding of the inhibitory effect of PPZ on the colony-forming potential of HNC cells, clonogenic assays were set up. Based on optimisation experiments, cisplatin and irradiation doses were chosen that when combined would not completely devastate the colony fractions. Considering the first three experimental groups (untreated, irradiation (IR) only and cisplatin only; Figure 7A), treatment with 0.5Gy IR resulted in a decreased fraction of colonies, with 78.08±11.9% clonal outgrowth, whereas 1.25μM cisplatin treatment produced 48.58+12.20% colony survival. Thus the 1.25μM concentration of cisplatin is more effective than 0.5Gy IR at reducing clonal outgrowth of FaDu cells. Cal27 cells showed a similar response pattern with 61.69±13.93% for IR only and 54.59+15.58%

for cisplatin alone. The colony number from cells treated with combined cisplatin and 0.5Gy IR was the lowest with 31.08±9.45% and 30.46±10.04% survival fraction for FaDu and Cal27 cell lines respectively. This combination was used as a positive control since cisplatin and IR are standard-of-care treatment for HNC.

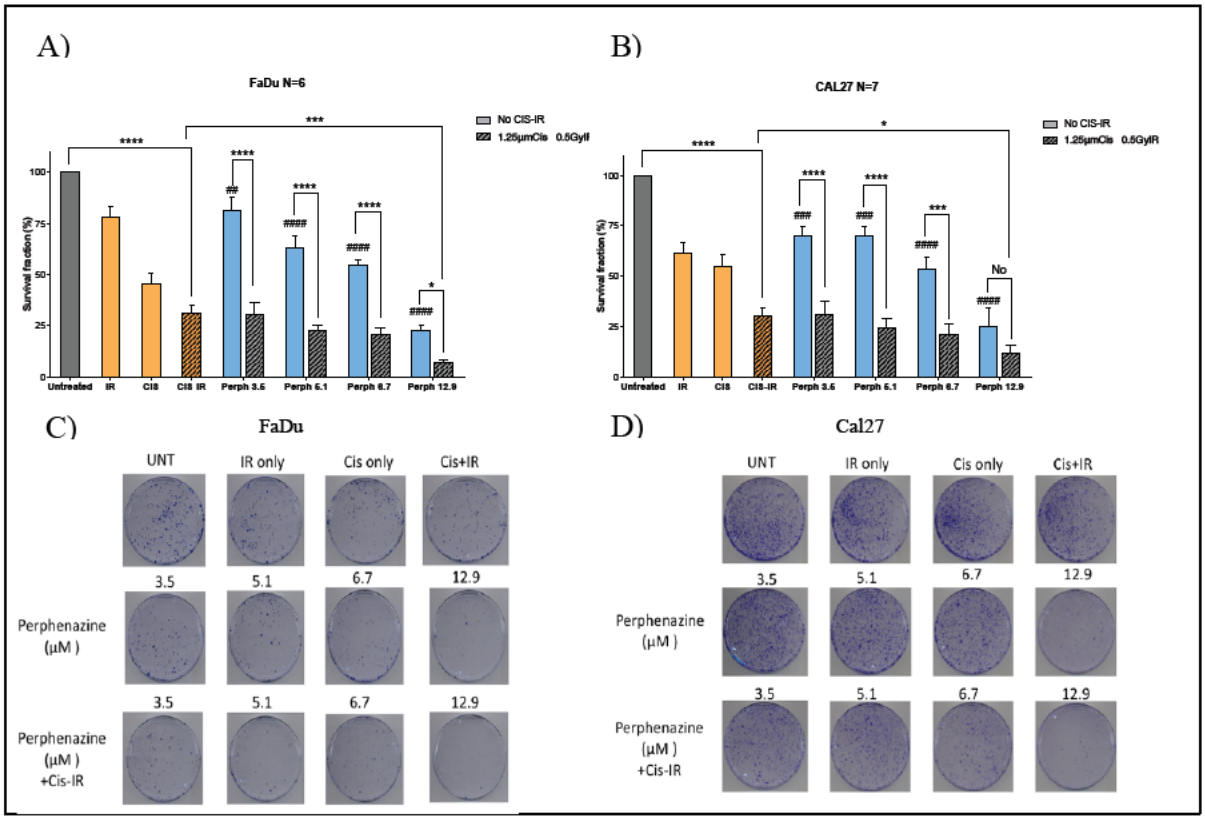


Figure 7: Clonogenic survival of FaDu (A) and Cal27 (B) cell lines exposed to increasing concentrations of perphenazine, with and without 1.25μM cisplatin and 0.5Gy irradiation (Cis+IR) for 24hours (N≥6). Values are presented as a percentage of untreated controls. Hatched bars indicate cells treated with 1.25μM Cisplatin and 0.5Gy IR; unhatched bars indicate no combination Cis + IR treatment. The blue bars represent treatment with PPZ only; orange bars represent the control group. Data are shown as the mean ±SEM. A two-way ANOVA with Dunnett's multiple comparison test was performed and p-values indicated on the graphs as follows: ##= p<0.01, ###=p<0.005, ####=p<0.001, which denote differences between PPZ only group and the untreated control; *=p<0.05, ***= p<0.005, ****=p<0.001. which denote differences between the treatments indicated. Representative images showing

clonogenic survival for FaDu(C) and Cal27(D) cells exposed to increasing concentrations of perphenazine for 24 hours, +/- Cis+IR.

PPZ only treatment (blue bars in Figure 7A), displayed a concentration-dependent effect on clonogenic survival for both FaDu and Cal27 cell lines: descending trend of colony number with increasing PPZ concentration from 3.5-12.9μM. The lowest concentration of PPZ (3.5μM) reduced the surviving fraction to 81.16±16.78% and 70.36±11.11% for FaDu and Cal27 cell lines respectively. At the highest PPZ concentration (12.9μM) surviving colony fractions (22.91±6.27% for FaDu, 25.30±23.50% for Cal27) were similar to the Cis + IR group (31.08±9.45% on FaDu; 30.46±10.04% on Cal27). In addition, PPZ treatment with Cis + IR displayed a concentration-dependent reduction of survival fraction.

In general, all groups treated with PPZ showed a significant concentration-dependent difference with untreated group (Figure7A and 7B: statistical data represented by #, FaDu: 3.5μM PPZ: p=0.0033; 5.1μM PPZ: p=0.0001; 6.7μM PPZ: p=0.0001; 12.9μM PPZ: p=0.0001; Cal27: 3.5μM PPZ: p=0.0009; 5.1μM PPZ: p=0.0009; 6.7μM PPZ: p=0.0001; 12.9μM PPZ: p=0.0001), indicating the inhibitory effect of PPZ on HNC cell proliferation. There is a significant difference between the PPZ only groups and the PPZ plus Cis-IR groups for both HNSCC cell lines (Figure7A and 7B: statistical data represented by *: FaDu: 3.5μMPPZ + cis-IR: p=0.0001; 5.1μM PPZ+cis-IR: p=0.0001; 6.7μM PPZ+cis-IR: p=0.0001; 12.9μM PPZ+cis:-IR p=0.012; Cal27: 3.5μM PPZ+cis-IR: p=0.0001; 5.1μM PPZ+cis-IR: p=0.0001; 6.7μM PPZ+cis-IR: p=0.0004;). Thus PPZ+cis-IR treatment is more effective than the PPZ only at inhibiting clonogenic survival. However, when comparing the PPZ+ Cis-IR and Cis-IR only groups, a significant difference was only observed for the highest concentration of PPZ (FaDu: p=0.0003; Cal27: p=0.043) on both HNSCC cell lines. A decreasing trend of survival was observed for the combination group with increasing concentrations of PPZ compared to standard-of-care (Cis-IR) for both HNC cell lines.

4.3 PPZ induces apoptosis of HNC cell lines

To further understand the mechanism of PPZ-induced cell death, Annexin V apoptosis assays were conducted on both FaDu and Cal27 cell lines. Cells were treated with various concentrations of PPZ (3.5μM, 5.1μM, 6.7μM, 12.9μM on FaDu; 3.5μM, 10μM, 12.9μM, 14.5μM on Cal27) +/- 2μM cisplatin for 48 hours, stained with Annexin V/PI and analysed by flow cytometry.

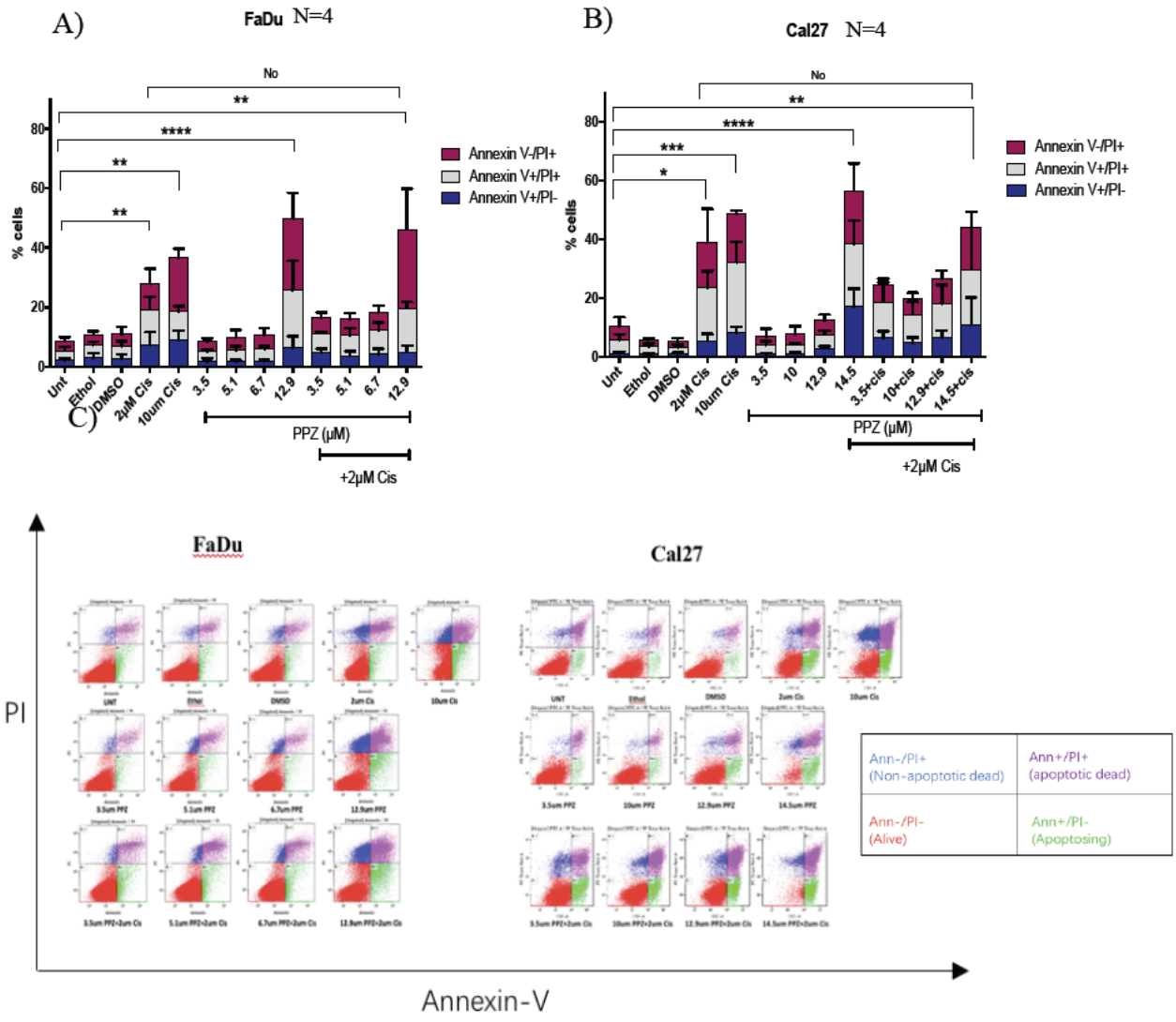


Figure 8: Assessment of FaDu (A) and Cal27 (B) apoptotic cell death following PPZ treatment with or without cisplatin (48-hour treatment, N=4). Various cell populations are indicated using the following colours: Annexin V+/PI- representing early apoptotic cells (blue), Annexin V+/PI+ representing apoptotic cell death (grey), Annexin V-/PI+

representing non-apoptotic cell death (maroon). Statistical significance of apoptotic cell death using two-way ANOVA with Dunnett's multiple comparison test is indicated by * stars as follows: ** =p<0.01, ****=p<0.001 between each treatment and the appropriate control (untreated (UNT) or 2μM cisplatin (Cis)). Data are presented as the mean ±SD. **(C) Representative dot plots demonstrating induction of apoptosis in FaDu and Cal27 cell lines treated with various concentrations of perphenazine alone or perphenazine with 2μM cisplatin (48-hours, N=4).** Apoptosis was detected by Annexin V and propidium iodide staining as described in Methods 2.4. Total apoptotic and cell death events were quantified and analysed using Kaluza 2.1.1 software and highlighted as: A-/- (Annexin -/PI -) (red), A+/- (green), A+/+ (purple), A-/+ (blue).

There is a significant difference between the group treated with cisplatin alone and the untreated group for both FaDu and Cal27 cell lines (Figure 8A and 8B: FaDu: 2μM cisplatin: p=0.004; 10μM cisplatin: p=0.008, Cal27: 2μM cisplatin: p=0.033; 10μM cisplatin: p=0.0004). Annexin V vs PI dot plots indicated induction of apoptosis (Annexin V+: A+/-, A+/+) when compared both groups exposed to the highest concentration of PPZ in the presence and absence of 2μM cisplatin with the control group (Figure 8C).

The graphs in figure 8A and 8B illustrate a concentration-dependent induction of apoptosis by PPZ; albeit non significantly at the lower concentrations. For FaDu cells, only the maximum concentration of PPZ (12.9μM) +/- 2μM cisplatin displayed statistical significance (12.9μM PPZ group: p=0.0001; 12.9μM PPZ+2μM Cis group: p=0.0032) compared to the untreated group. The Cal27 cell line (Figure 8B), appeared insensitive to concentrations of PPZ ≤12.9μM. Only the highest concentration of PPZ (14.5μM) +/- 2μM cisplatin presented a significant difference in apoptotic cell populations (only PPZ: P=0.0001, PPZ+2μM cisplatin: p=0.0015) when compared to the untreated group. No statistical difference in apoptotic populations was observed for any concentration of PPZ plus 2μM cisplatin versus 2μM cisplatin alone on FaDu or Cal27 cell lines, thus no synergistic effect on apoptosis is apparent between PPZ and cisplatin.

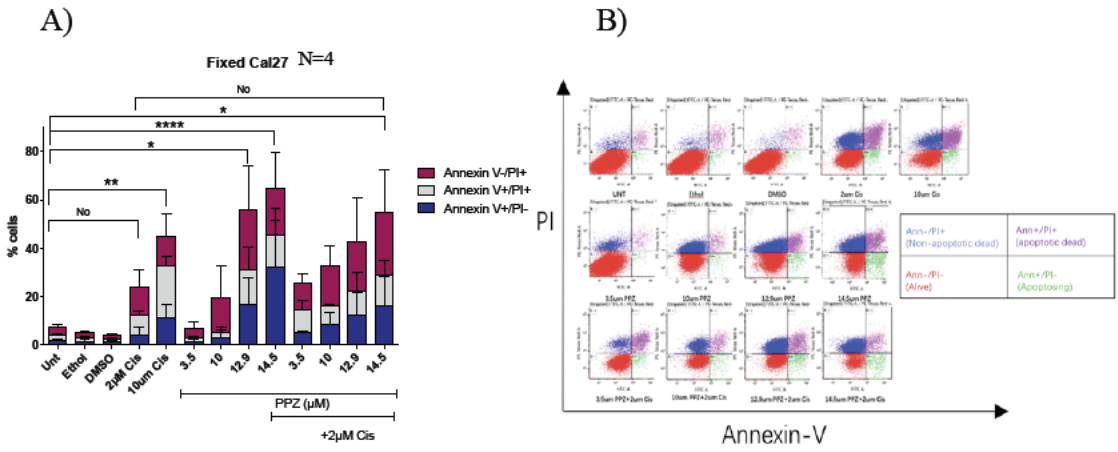


Figure 9: (A) Annexin V assay demonstrating a PPZ concentration-dependent effect on apoptosis of fixed Cal27 cell lines (48hour treatment, N=4). Various cell populations are indicated using the following colours: Annexin V+/PI- representing early apoptotic cells (blue), Annexin V+/PI+ representing apoptotic cell death (grey), Annexin V-/PI+ representing non-apoptotic cell death (maroon). Statistical significance of apoptotic cell death using two-way ANOVA with Dunnett's multiple comparison test was represented by * stars as follows: * =p<0.05, ** =p<0.01, ****=p<0.001, data are shown by the mean ±SD. **(B) Representative dot plots demonstrating induction of apoptosis on fixed Cal27 cell lines treated with various concentrations of perphenazine alone or perphenazine with 2μM cisplatin (48-hours, N=4).** Total apoptotic and death events were quantified and analysed using Kaluza 2.1.1 software and highlighted as: A-/- (Annexin -/PI -) (red), A+/- (green), A+/+ (purple), A-/+ (blue).

Due to the LSR-II flow cytometer frequently being out of order, the fixation of Cal27 cell lines following PPZ treatment was evaluated (Figure 9), in an attempt to overcome any last-minute technical issues. As shown in figure 9A, a concentration-dependent increase in apoptotic cell populations (Annexin V +) was observed for both the PPZ alone and PPZ with cisplatin groups. Following fixation, significant differences in Annexin V positivity were observed for the 12.9μM (p=0.012) and 14.5μM PPZ (p=0.0001) groups, again suggesting that PPZ induces apoptosis. The highest concentration of PPZ (14.5μM) with cisplatin group,

also showed significance compared with the untreated group with p=0.03. However, the addition of 2μM cisplatin did not improve the efficacy of the apoptotic cell population, especially at higher PPZ concentrations of 12.9μM and 14.5μM. No significant difference between any PPZ alone and the corresponding PPZ with cisplatin group was observed for fixed Cal27 cells (Figure 9A).

In terms of the dot plot for fixed Cal27 cells, (Figure 9B), there is an unexpected gap between the live (red) and non-apoptotic cell death (blue) populations, especially for PPZ treated cells. To understand why this gap appears, the results for fixed Cal27 cells (Figure 9A) were compared with the fresh Cal27 cells (Figure 8B). All control groups except for 2μM cisplatin showed a similar proportion of apoptotic cell death in fixed and unfixed populations. However, PPZ alone groups presented a different proportion changing on the cell population. A higher proportion of non-apoptotic cell death (Annexin negative/ PI positive) in each PPZ group was illustrated in figure 9A (maroon group). According to the statistical analysis, the 14.5μM PPZ group with or with cisplatin demonstrated a significant difference compared to the untreated group (14.5μM PPZ alone: p=0.0001; 14.5μM PPZ with cisplatin: p=0.03). No significant difference was observed between 14.5μM PPZ with 2μM cisplatin and 2μM cisplatin alone group. All the data described above were similar to those observed using fresh Cal27 cells (14.5μM PPZ alone: p=0.0001; 14.5μM PPZ with cisplatin: p=0.0015). The difference is that in the fixed cell assay 12.9μM PPZ treatment resulted in a statistical difference with p=0.012, whereas there no difference was observed in the fresh cell assay. Also, there was no difference between untreated cells and the 2µM cisplatin treated cells in the fixed assay. Therefore, I have accepted the results as an effect of the treatment and not the experimental set up.

4.4 PPZ alters LC-3 II/LC-3 I expression in HNSCC cell lines

Five proteins were selected for investigating the potential mechanism of action for the observed effects of perphenazine on FaDu cells:LC-3, p53, p21, AKT and phosphorylated

(p)AKT. P53 is the most frequently mutated gene in HNC as mentioned before (**1.3.3 Molecular biology of head and neck cancer**), and it modulates various signalling pathways, such as cell cycle arrest by targeting P21 and apoptotic cell death. Due to the mutation of p53 in FaDu cell lines, p21 as the downstream target of p53 was investigated to evaluate the activity of p53. It was demonstrated before that Akt, a serine/threonine specific protein kinase associated with cell proliferation pathway, can be inactivated due to PPZ induced dephosphorylation by targeting PP2A (**2.5 Perphenazine**). Therefore, the ratio of pAkt/Akt could indicate not only the activity of AKT related signalling pathway, but also the potential possibility of PP2A as the PPZ target candidate in head and neck cancer. LC-3, as an indicator of autophagy was selected for this study due to that PPZ was identified to affect autophagy flux by increasing LC3-II and P62 expression (Kuzu, Gowda, Noory, & Robertson, 2017).

Three independently repeated treatment samples were used for protein detection, but only LC-3 expression displayed a significant difference after 10μM PPZ treatment compared to the control group (P=0.015). As it was shown on figure10, a concentration-dependent accumulation of LC-3 II/LC-3 I was observed through Western blot, indicating that PPZ affects autophagy by inducing autophagosome formation in HNSCC cell line. In addition, there is no difference between 7μM PPZ group and PPZ with cisplatin group. Addition of cisplatin did not affect PPZ induced autophagosome formation.

To determine the effect of PPZ on phosphorylation, the pAkt/Akt levels were selected for proportional analysis by Western blot. According to the statistical analysis, there is no significant difference between treatment group and control group. However, there is a concentration-dependent decrease in expression with PPZ treatment (Figure 10). This indicates that PPZ could decrease the phosphorylated proportion of AKT expression with increasing concentrations. Compared to the expression of β-actin, p53 expression (cell cycle regulator) did not appear to show any difference between the different treatment groups, and p21 (cyclin-dependent kinase inhibitor) neither.

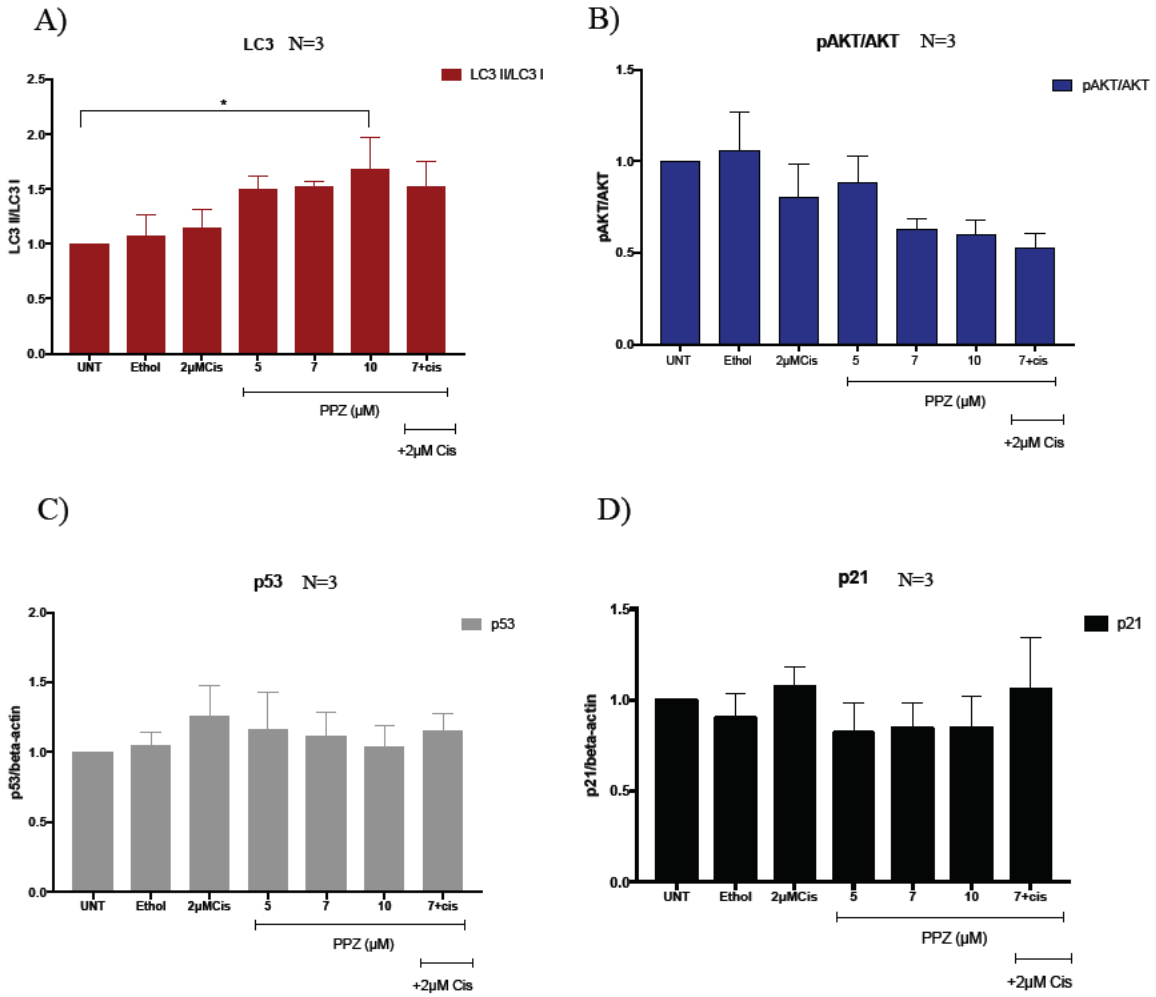

A)
LC3 N=3
LC3 II/LC3 I
LC3 II/LC3 I
UNT
Ethol
2μMCis
5
7
10
7+cis
PPZ (μM)
+2μM Cis
B)
pAKT/AKT N=3
pAKT/AKT
pAKT/AKT
C)
p53 N=3
p53
p53/beta-actin
D)
p21 N=3
p21
p21/beta-actin
E)
PPZ (μM)
UNT
Ethol
2μM Cis
5
7
10
7+ Cis
LC3
β-actin
pAKT
β-actin
p53
p21
AKT
β-actin

Figure 10: Western blot analysis of pAKT, LC3 following 24 hours perphenazine or cisplatin treatment and appropriate controls (N=3). Histograms representing the quantitative changes in LC3 (A), pAKT (B), p53 (C), p21(D) normalised to an untreated control. Values generated by densitometry analysis using ImageJ. Statistical significance calculated by a one-way ANOVA followed by Dunnett's multiple comparisons test. *Stars indicate P-values on the graphs as follows: *=p<0.05. (E) Western blots showing increase of LC3 and decrease of pAKT(left to right) following 24-hour exposure to increasing concentrations of PPZ (5, 7, and 10 μM), alongside 2 μM cisplatin alone and in combination of 7 μM PPZ . Loading control β-actin.

4.5 Cell cycle analysis with PPZ treatment HNC cell line

According to the reported mRNA sequence data in literature PPZ treatment in melanoma cancer, I did a gene ontology analysis and found PPZ could deregulate cell cycle related genes (supplementary Table1). To understand the relationship between PPZ and head and neck cancer, cell cycle assay with 48hrs PPZ treatment was conducted in Cal27 cell lines. Sub-G1 represents a broad hypodiploid DNA content, indicating apoptotic cell, nuclear fragments, and some necrotic cell. G1 phase with normal (diploid) DNA content is the initiation of cell cycle regulated by G1 checkpoint. S phase refers to DNA synthesis and G2 phase regulated by G2 checkpoint is the last step before mitosis.

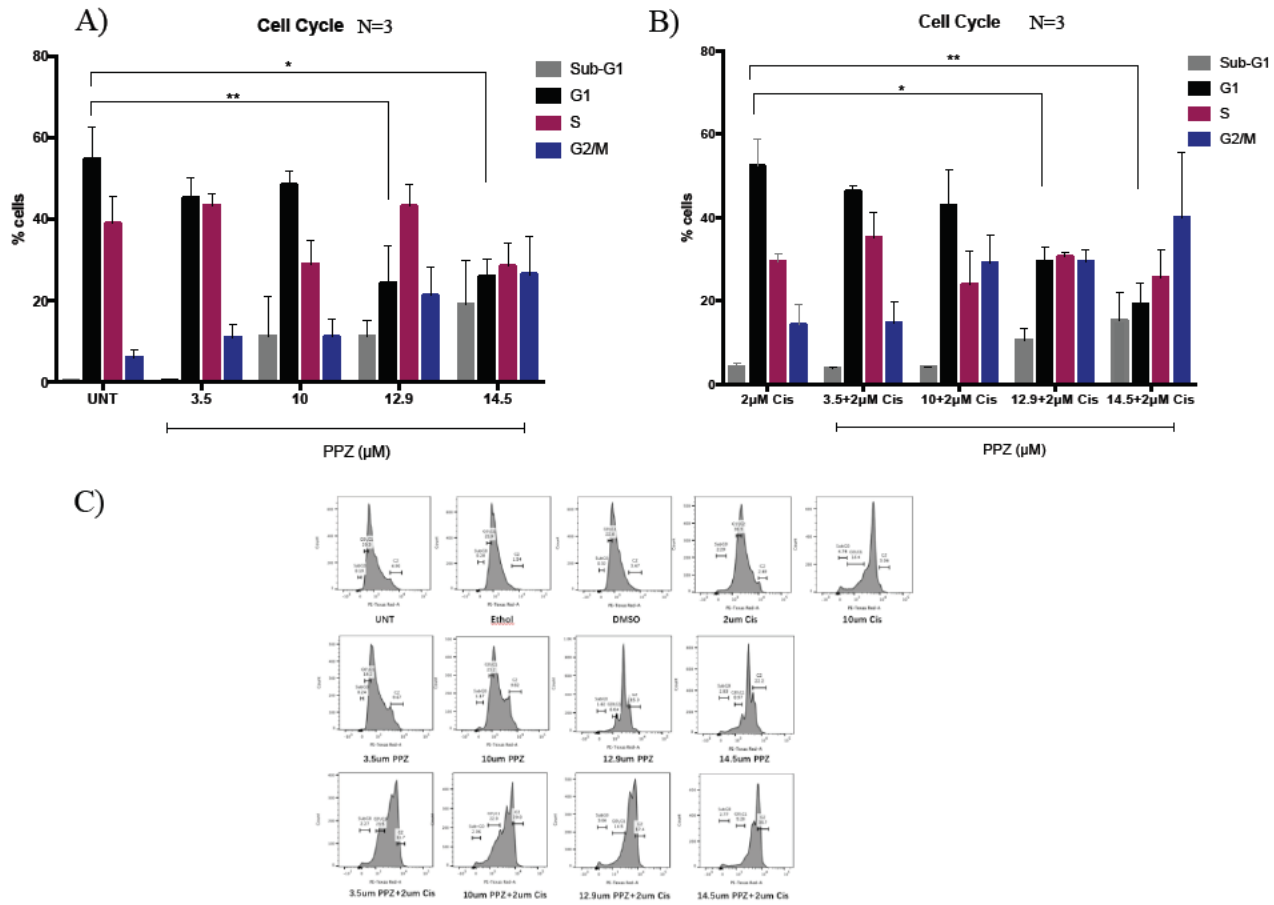


Figure 11: Cell cycle assay indicating that PPZ promotes G1 to S transition in Cal27 Cell lines with A) only PPZ treatment and B) PPZ and 2μM cisplatin treatment (N=3). C) Cell cycle histogram. Statistical significance calculated by a two-way ANOVA followed by Dunnett's multiple comparisons test. *Stars indicates P-values on the graphs as follows: *=p<0.05, **=p<0.01. Sub-G1, G1, S, G2/M phases were represented by the colour grey, black, red and blue respectively.

There is a concentration dependent increase of the frequency of Sub G1 in cell cycle in PPZ treatment group (Figure 11A and supplementary Figure1A), indicating that PPZ induce cell death. However, there is no statistical difference in Sub -G1 assay (supplementary Figure1A). A significant difference between untreated group and PPZ group was observed in G1 phase (12.9μM PPZ group: p=0.006; 14.5μM PPZ group: p=0.01), showing that PPZ could be promotingG1 to S cell cycle transition in HNC cell lines. The addition of cisplatin in PPZ

group represented a similar reduction (12.9μM PPZ group: p=0.046; 14.5μM PPZ group: p=0.003) as the only PPZ group displayed in cell cycle G1 phase, indicating that the addition of cisplatin does not inhibit PPZ's ability to promote G1 to S transition (Figure 11B and supplementary Figure 1B). An increasing frequency of G2/M with increasing concentration of PPZ compare to the untreated group (14.5μM PPZ group to untreated group: 26.47±9.19% to 5.95±1.99%) could be observed in the G2/M bar chart and histogram (Figure 11A and supplementary Figure 1D), indicating the cell cycle process could be blocked in G2/M phase with PPZ treatment; no statistical significance was established. Overall, we observe a trend of concentration dependent transition from G0/G1 phase to G2/M phase with PPZ. More importantly this appears to facilitate the 2μM effect we observe on the cell cycle.

5. Discussion

Perphenazine was identified following high throughput screening of the Prestwick library. The aim of this project was to validate the initial findings and to investigate the potential of PPZ to be used as a candidate drug for HNC treatment. In order to do this, I aimed to complete an *in vitro* validation on both FaDu and Cal27 cell lines, and to begin the investigation on the mechanism of action of PPZ against HNC. All my results illustrated the promising anti-cancer effect of PPZ on HNC cell lines as evidenced by reduced cell viability, inhibition of colony formation and induction of apoptotic cell death. In addition, PPZ was shown to influence autophagy by increasing the accumulation of LC-3 II and an increase in LC3-II/LC3-I. PPZ in the presented study also was shown to affect cell cycle, reducing the percentage of cells in G0/G1 phase and potentially by blocking transition to mitosis (G2 to M phase). This can be enhanced when cells were also exposed to 2μM cisplatin, indicating a potential benefit to administer PPZ following chemotherapy treatment to enhance DNA damage leading to cell death. However, additional cell lines and primary patient cells are required for a more in-depth assessment to fully understand this effect and its impact in the progression of PPZ as a potential therapeutic option.

5.1 PPZ induces apoptosis in HNC cell lines

Perphenazine's ability to induce apoptosis of cancer cells has been previously identified and reported. Firstly, it was demonstrated that PPZ-induced apoptosis is mediated by PP2A (Gutierrez et al., 2014). As an activator of PP2A, PPZ could facilitate dephosphorylation of PP2A substrates like pBAD, the pro-apoptotic BCL2 family member, thus triggering apoptosis. Secondly, Bax and Bcl-2 were suggested to play an important role in PPZ-induced cell death. Knockdown of Bax or overexpression of Bcl-2 could block cancer cell death after PPZ treatment (Gutierrez et al., 2014; Kuzu et al., 2017). In addition, the investigators demonstrated that inhibition of apoptosome formation in parallel with PPZ treatment led to a significant increase in cell viability. This suggests that PPZ promotes apoptosome activity, resulting in apoptotic cell death (Kuzu et al., 2017). As I demonstrate in figure 12, when the mitochondrial apoptotic pathway is activated, pro-apoptotic Bcl family members are engaged,

leading to mitochondria permeability and apoptosome activity. All the above suggest that PPZ-mediated cell death is associated with mitochondrial function; however, whether it is caspase-dependent still needs further investigation.

It was reported that PPZ mediates caspase-dependent cell death in leukemia, whereas it induces caspase independent cell death in melanoma (Figure 12). Hence, the effect appears to be dependent on cell type. No PPZ-induced apoptotic mechanism has been reported in HNC to date. My current study only demonstrated that PPZ can induce apoptosis at higher concentrations in HNC, and its mechanism of action is still not fully elucidated.

It was identified that small molecule activators of PP2A (SMAPs) derived from the phenothiazine family mediated caspase-dependent cell death, and this was also associated with increased poly(ADO-ribose) polymerase (PARP) cleavage (Sangodkar et al., 2017). These data are consistent with a model in which PPZ induces mitochondrial associated apoptosis mediated by PP2A in HNC. Further experiments are needed to explore this mechanism.

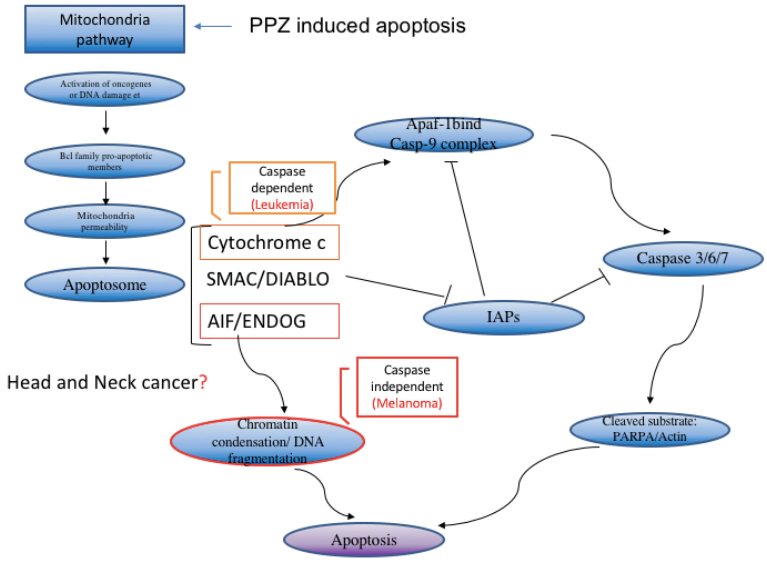


Figure 12: Reviewed and summarized mitochondrial apoptotic pathway associated with perphenazine.

In my work, apoptotic cell death was only induced above control levels at the highest concentration of PPZ (FaDu: 12.9μM PPZ alone: p= 0.0001; Cal27: 14.5μM PPZ alone: p=0.0001) indicated that apoptosis was induced by PPZ in a not as expected concentration dependent manner, at the range assessed. However, a concentration-dependent apoptosis was demonstrated for leukaemia and endometrial cancer *in vitro* with different concentration of PPZ, 10 – 30 μM (Chen et al., 2020; Gutierrez et al., 2014). It is possible that PPZ shows variable efficiency on different cancers, or even cell lines with different associated mutations. There is no statistical difference between the 2μM cisplatin group and all PPZ concentrations in the presence of 2μM cisplatin group on both FaDu and Cal27 cell lines. However, the PPZ with 2μM cisplatin group displayed an inhibitory effect on apoptotic cell population compared to the only PPZ group, however this was not statistically significant. In terms of cell cycle sub-G1 histogram (supplementary Figure 1A), it also displayed a similar inhibitory result that a reduction could be observed from only PPZ group to PPZ with cisplatin group. Both of these experiments indicate that cisplatin may impede PPZ induced apoptotic signalling pathway, but further investigation is required. The mode of action of cisplatin is to induce DNA damage, leading to activation of damage recognition proteins via multiple signalling pathways, such as MAPK (Erk, Jnk, p38), p53, p73 (Siddik, 2003). Among them, activation of p38/JNK will ultimately activate FasL induced apoptosis. The apoptosis mechanism of PPZ is unclear, but as mentioned previously appears to involve PP2A in leukaemia (Gutierrez et al., 2014). The function of PP2A is to dephosphorylate its substrates like Jnk. It was identified that PP2A inhibitor could over activate JNK pathway inducing repression of cell growth in cancer (Gong et al., 2015). In addition, LB100, an inhibitor of PP2A, was demonstrated that it could enhance the efficacy of cisplatin, overcome cisplatin resistance, and promote cisplatin induced apoptosis in several cancers (Ho et al., 2016; Uddin et al., 2020). The mechanism between cisplatin and PP2A in apoptosis is still not clear. I think it merits further study to explore the cisplatin resistance and PP2A function in cancer, as this is a complex molecular pathway with pro and anti-apoptotic networks.

5.2 PPZ increases LC3 expression in head and neck cancer

Autophagy is a cellular degradation process, which via phagophore, autophagosome, and autolysosome formation, recycles cellular components, protects against damage or modulates cell death. It plays dual roles in cancer development: promotion and inhibition. Perphenazine is a drug originally designed to target dopamine receptors as an antagonist to treat psychotic disorders (**2.5 Perphenazine**). Many dopamine D_2 receptor (D_2R) antagonist drugs demonstrated an ability to induce autophagy, like trifluoperazine, thioridazine, and pimozide. The PI3K/mTOR pathway was suggested to have a partial role in autophagy (Weissenrieder, Neighbors, Mailman, & Hohl, 2019). However, Kuzu et al. (2017) described a concentration-dependent expression of LC3-II (autophagosome protein) and p62/SQSTM1(cargo protein, self-degradation before autolysosome formation) with PPZ treatment. High expression of both LC3-II and p62 indicated that PPZ inhibits autophagy flux in cancer. To understand the relationship between PPZ and autophagy in HNC, protein expression with PPZ treatment was investigated via Western blot. PPZ promoted LC-3 II expression (leading to an increased LC-3 II/LC-3 I ratio) and potential aggregation of autophagosomes, as demonstrated by Kuzu et al. (2017). Thus, I hypothesize that PPZ can block the autophagic flux and prevent completion of autophagy in HNC cell lines, as described by Kuzu et al. (2017) for melanoma cells. Further studies could focus on investigating the potential effects of PPZ treatment on p62 expression in HNC, to understand more about the relationship between PPZ and autophagy.

5.3 PPZ treatment and cell cycle in head and neck cancer

Currently, no study has reported the relationship between PPZ and cell cycle. However, PP2A, a potential target of PPZ, was identified as a key regulator in cell cycle via its phosphatase function. In the cell cycle process, checkpoints ensure that cells are ready for entry to the next phase. As a master checkpoint protein of G1 to S transition, Rb is regulated by PP2A (Wlodarchak & Xing, 2016). Phosphorylation modulation of Rb will promote cells to pass the G1-S checkpoint to DNA synthesis. Therefore, there is a significant reduction of G1 proportion in PPZ-treated cells compared to the untreated group (Figure11A and

supplementary Figure 1B). PP2A-PR70 holoenzyme has been shown to modulate Cdc6 (cell division control protein 6) in cell cycle (Wlodarchak & Xing, 2016). Although when and where Cdc6 will be dephosphorylated by PP2A is not clear, DNA synthesis is demonstrated to be regulated by PP2A. Wlodarchak and Xing (2016) suggested that PP2A is a gatekeeper for mitosis. Mitotic entry requires inhibition of PP2A. Meanwhile, PP2A-B55 holoenzyme is inactivated in this process. Therefore, if PPZ could activate PP2A function, especially PP2A-B55, then mitotic entry will be blocked. My results, as illustrated on the G2/M histogram, are consistent with this but further work is required. Overall, PPZ can promote G1 to S transition, potentially affects DNA synthesis and appears to block cell entry into mitosis in HNC cell lines.

5.4 PP2A is the potential target of PPZ in head and neck cancer

Clonogenic assays on FaDu and Cal27 cell lines, showed a concentration-dependent inhibition of colony survival at lower PPZ concentrations (3.5μM to 6.7μM), suggesting that a lower concentration of PPZ inhibits cell proliferation. However, according to the apoptotic assay, only the highest concentration of PPZ could induce apoptosis. Therefore, I hypothesize that lower concentrations of PPZ (less than 6.7μM) can suppress HNC cell line proliferation; higher concentrations (greater than 12.9μM), can lead to additional effects like inducing cell death through apoptosis.

It was demonstrated that SMAPs could inhibit cell growth and induce apoptosis in lung cancer. Investigators developed phenothiazine-derived SMAPs suggesting a biphasic response in cancer (Sangodkar et al., 2017). PPZ and these developed SMAPs are from the same drug class and they demonstrate similar anticancer responses. Additionally, intracellular cholesterol transport was shown to be inhibited by PPZ (Kuzu et al., 2017) and SMAPs. This can have an impact on cell metabolism, cell cycle and drug interactions. Low density lipoprotein (LDL) associated cholesterol biosynthesis was upregulated by PPZ treatment (Kuzu et al., 2017). PP2A is required for LDL uptake by binding to SREBF, a cholesterol

biosynthesis regulation gene (Rice et al., 2014). This implicates lipid biosynthesis as a further potential mechanism of action.

All these studies provide reasonable support to the hypothesis that PP2A is the potential target of PPZ in HNC.

PP2A is a serine /threonine phosphatase involved in normal cell growth and development, but it is frequently inactivated in cancer due to the high expression of its inhibitors, such as SET and CIP2A. It is composed of a dimeric core enzyme - the structural A and catalytic C subunits – which are supported by a regulatory B subunit, forming a hetero-trimer; each subunit comprises many isoforms. Due to the structural diversity of holoenzymes, over 300 substrates are regulated by PP2A (Wlodarchak & Xing, 2016). Some studies have shown that inhibitors of PP2A can impede tumour growth indicating that PP2A is likely to play a key role in several cancer due to its different dephosphorylation modulation on a number of substrates (Kiely & Kiely, 2015). Conversely, activation PP2A has been investigated as a therapeutic approach in many cancers (Mazhar, Taylor, Sangodkar, & Narla, 2019; O'Connor, Perl, Leonard, Sangodkar, & Narla, 2018). Activation of PP2A could inhibit multiple signalling pathways important for cancer development. Gutierrez et al. (2014) have demonstrated that PPZ can activate PP2A by direct binding to subunit A alpha, inducing de-phosphorylation of PP2A substrates. As a scaffolding (A) subunit holding C and B subunit, there are 15 Huntington-elongation-A-subunit-TOR (HEAT) repeats in the PP2A subunit A. Subunit C could bind to HEAT 11-15, becoming the PP2A A-C dimer. Only PP2A C subunit contains active site for PP2A activation. However, conformational changes on PP2A A subunit when binding to other subunit could activate PP2A function (Wlodarchak & Xing, 2016). SMAPs derived from phenothiazine study suggested that these SMAPs could binding to the HEAT repeat domains in PP2A A subunit and induce a conformational change (Sangodkar et al., 2017). The residues K194 and L198 in the subunit A of PP2A were identified as a drug-binding site in these SMAPs treatment study (Sangodkar et al., 2017). Additionally, Ramaswamy, Spitzer, and Kentsis (2015) also mentioned that PPZ could induce an allosteric effect on PP2A activity when it binds to the A scaffold HEAT domains. An *in*

silico docking study as a future investigation could allow for an insight of the potential interaction of PPZ in this binding pocket. Therefore, the study on PP2A activity with PPZ treatment and the conformational changes of PP2A could be investigated in HNC cancer to further develop our mechanistic understanding.

Focusing on the PPZ inhibitory effect on cell proliferation, I summarised the common cell proliferation pathways in HNC, such as RAS/MAPK/PI3K related pathway, and combined this with data from the literature detailing proteins that are de-phosphorylated following PPZ treatment, such as Akt, ERK and Myc. Most of these proteins are associated with PP2A function. A potential PPZ-induced signalling pathway is presented in figure 13 with my hypothesis that PPZ activates PP2A to inhibit MAPK signalling pathway.

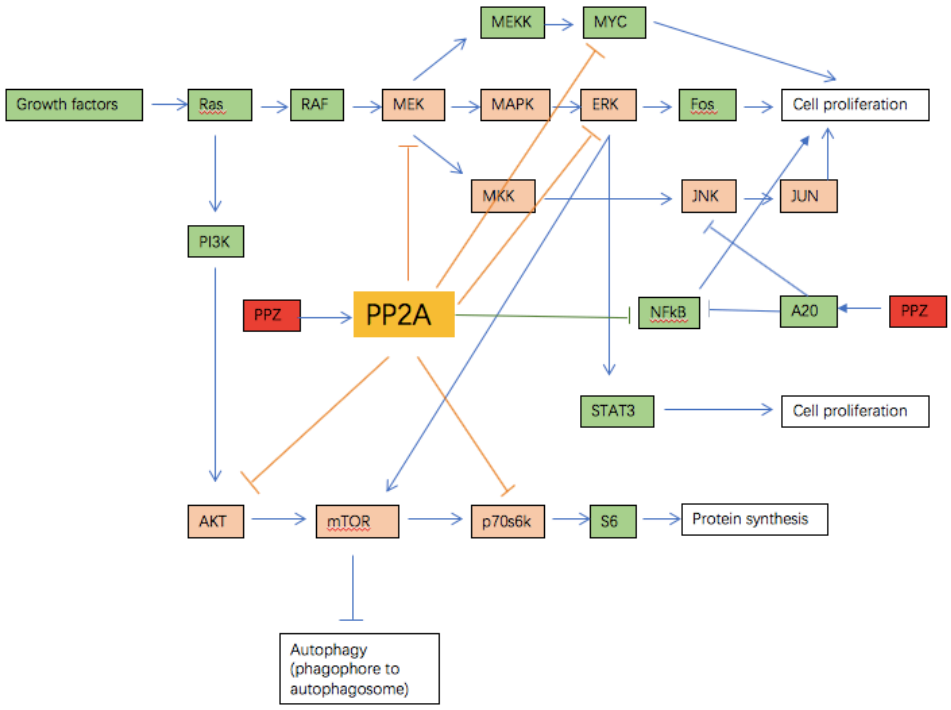


Figure 13: Novel signalling pathway of PPZ induced through PP2A activity inhibiting cell proliferation. Genes highlighted by the pink colour could be affected and tracked on the MAPK signalling pathway.

5.5 Limitations and opportunity for further study

The achievable clinical concentration of PPZ in psychosis treatment is around 12.37μM (5mg per 1ml, Trilafon® instruction, a brand of perphenazine). This safe concentration of PPZ is similar to IC_{50} values obtained from PPZ concentration-response curves for both Cal27 and FaDu cell lines (Cal27:11μM, FaDu: 11.9μM). In any future development, it is better to keep the PPZ concentration close to the clinically indicated value to minimise side effects. The central nervous system (CNS) related side effects must be considered in any future clinical work. A nanoliposomal encapsulation of PPZ was demonstrated to reduce CNS-related side effects and enhance therapeutic activity *in vivo* (Kuzu et al., 2017). This may be relevant for clinical studies if higher concentrations of PPZ are needed to mediate anti-cancer effects. Commercial cancer cell lines are a stable and easy platform for studying drug cytotoxicity, providing a valuable model for preliminary studies. However, they cannot fully represent the real environment *in vivo*. Although cell lines have a higher reproducibility with uniform cell type, changes in phenotype, functional alterations and altered genomic content is inevitable with extensive passaging. For this reason, we validated both cell lines before and after my work. The cell signalling conduction *in vivo* also cannot be fully represented by cell lines due to its loss of polarity and lack of key morphology features. Therefore, further investigation using human primary cells and 3D cultures (such as organoids) is needed to confirm the potential mechanism identified from cell lines. Primary cell lines derived from patient tissues retain characteristics of morphology and phenotype, whereas commercial cell lines may display different molecular features (Bryant et al., 2019; Pastor et al., 2010). Organoids from primary cell lines provide a more elaborate model *in vitro* drug discovery, more closely resembling the cellular organisation and behaviour of the organism. Compared to animal experiments, organoids also can reduce the complexity of experiments and are suitable for real-time imaging techniques (Kim, Koo, & Knoblich, 2020). Therefore, organoids could be a good model to assess PPZ efficacy and mechanism in cancer.

In addition, the effects of PPZ treatment on normal non-cancer cells needs to be investigated with PPZ treatment to assess the 'off-target' cytotoxicity of PPZ. However, perphenazine is a

licenced drug used for decades in clinical practise, therefore we do not expect any such toxicities.

It has been identified that HPV infection will affect head and neck cancer development and the efficacy of drug treatments (**2.2.2 Aetiology**). In this project, both Cal27 and FaDu cell lines are HPV negative cell lines. Whether HPV positive cell lines will be similarly affected by PPZ needs further study. If PP2A indeed regulates Rb this could provide a differential response in HPV+ cell lines as E7 can target Rb too. A number of well characterised cell lines and models exist to allow for this effect to be explored in the future.

Western blot results from my preliminary studies indicated that PPZ will decrease phosphorylation of Akt, but no significant difference was observed following 24-hour exposure. Assessment of protein phosphorylation reactions at a single time point may miss key changes, especially as the timing of protein phosphorylation varies for different drug concentrations. It was demonstrated that 15 minutes of PPZ treatment over 10μM could dephosphorylate pAKT in leukaemia (Gutierrez et al., 2014). All the other studies also demonstrated that PPZ induced dephosphorylation with less than 6 hours treatment at concentrations higher than 10μM (Palanichamy et al., 2017; Tsuji et al., 2016). Therefore, further study with various treatment times associated with higher concentration of PPZ may present a more accurate result. Additionally, Western blot only provides a semi-quantitative analysis of protein expression and analysis is complex for proteins with similar or same molecular weight. It is also time-consuming and laborious. Thus, multicolour fluorescence imaging and/or mRNA sequence analysis may be better methods for rapid and in-depth study of the molecular mechanism of PPZ against HNC. However, Western blot is still a valuable technique as it can provide us with results that can be further investigated using alternative assays.

Cell cycle assays suggested that PPZ may impede cell cycle transition in G2/M phase blocking entry to mitosis. However, statistical analysis showed no significant difference

between the PPZ and untreated groups. The cell cycle is a dynamic process. To improve the accuracy of the assay, allow comparison of results between different samples /time points and improve reproducibility, chick erythrocyte nuclei (CEN) could be used as an internal control in the future. My raw data in each phase of cell cycle are not very clear. This assay requires further optimisation of experimental conditions and an increased number of cell lines/ conditions to fully explore the potential effects of PPZ.

6. Conclusion

In summary, PPZ has been identified as a potential candidate drug against HNC. PPZ reduces cell viability (~50%) at clinically achievable concentrations (12.37μM; Trilafon® , a brand of perphenazine), and in a concentration-dependent manner (from 5μM to 30μM) on both FaDu and Cal27 cell lines. PPZ not only inhibits colony formation, in a concentration-dependent manner (<12.9uM), but also induces apoptosis at a higher concentrations (FaDu: 12.9uM; Cal27: 14.5uM). In addition, PPZ was shown to affect autophagy by increasing ratio of LC3-II/LC3-I expression and promotes G1 to S transition in cell cycle. PPZ may also block cell cycle in G2/M phase. All the results in this report, including the dephosphorylation of pAKT, indicate that PP2A is the potential target of PPZ in HNC; hence this pathway merits further investigation.

In the future, the details of how PPZ inhibits HNC cells need to be explored, and its potential target(s) elucidated further.

7. Acknowledgement

I would like to express my deep gratefulness to all the people who helped me at InHANSE throughout this study. Many Thanks to their endless patience, understanding and kindness. I would particularly like to thank Gordan Ryan for his great support in lab techniques involved in this project. Endless appreciation goes to Dr Nikos Batis, Dr Rachel Spruce and Dr. Jill Brooks for their invaluable and inspiring guidance. I would also like to express my sincere acknowledgement to Prof. Hisham Mehanna for overseeing the development of this project.

8. Reference

Anand, P., Kunnumakkara, A. B., Sundaram, C., Harikumar, K. B., Tharakan, S. T., Lai, O. S., Aggarwal, B. B. (2008). Cancer is a preventable disease that requires major lifestyle changes. *Pharm Res, 25*(9), 2097-2116. doi:10.1007/s11095-008-9661-9

Ashburn, T. T., & Thor, K. B. (2004). Drug repositioning: identifying and developing new uses for existing drugs. *Nat Rev Drug Discov, 3*(8), 673-683. doi:10.1038/nrd1468

Brana, I., & Siu, L. L. (2012). Locally advanced head and neck squamous cell cancer: treatment choice based on risk factors and optimizing drug prescription. *Ann Oncol, 23 Suppl 10*, x178-185. doi:10.1093/annonc/mds322

Bray, F., Ferlay, J., Soerjomataram, I., Siegel, R. L., Torre, L. A., & Jemal, A. (2018). Global cancer statistics 2018: GLOBOCAN estimates of incidence and mortality worldwide for 36 cancers in 185 countries. *CA Cancer J Clin, 68*(6), 394-424. doi:10.3322/caac.21492

Bryant, J., Batis, N., Franke, A. C., Clancey, G., Hartley, M., Ryan, G., Mehanna, H. (2019). Repurposed quinacrine synergizes with cisplatin, reducing the effective dose required for treatment of head and neck squamous cell carcinoma. *Oncotarget, 10*(50), 5229-5244. doi:10.18632/oncotarget.27156

Cancer Research UK. Retrieved from https://www.cancerresearchuk.org/health-professional/cancer-statistics/worldwide-cancer#heading-Zero

Castilho, R. M., Squarize, C. H., & Almeida, L. O. (2017). Epigenetic Modifications and Head and Neck Cancer: Implications for Tumor Progression and Resistance to Therapy. *Int J Mol Sci, 18*(7). doi:10.3390/ijms18071506

Chaturvedi, A. K., Anderson, W. F., Lortet-Tieulent, J., Curado, M. P., Ferlay, J., Franceschi, S., Gillison, M. L. (2013). Worldwide trends in incidence rates for oral cavity and oropharyngeal cancers. *J Clin Oncol, 31*(36), 4550-4559. doi:10.1200/jco.2013.50.3870

Chen, Y., Cui, Y., Sun, X., Wu, H., Ou, M., Tang, Y., Li, J. (2020). Repurposing of antipsychotics perphenazine for the treatment of endometrial cancer. *Bioorg Med Chem Lett, 30*(14), 127239. doi:10.1016/j.bmcl.2020.127239

Cunningham, F. H., Fiebelkorn, S., Johnson, M., & Meredith, C. (2011). A novel application of the Margin of Exposure approach: segregation of tobacco smoke toxicants. *Food Chem Toxicol, 49*(11), 2921-2933. doi:10.1016/j.fct.2011.07.019

Dok, R., & Nuyts, S. (2016). HPV Positive Head and Neck Cancers: Molecular Pathogenesis and Evolving Treatment Strategies. *Cancers (Basel), 8*(4). doi:10.3390/cancers8040041

Forastiere, A. A., Ang, K., Brizel, D., Brockstein, B. E., Dunphy, F., Eisele, D. W., Yueh, B. (2005). Head and neck cancers. *J Natl Compr Canc Netw, 3*(3), 316-391. doi:10.6004/jnccn.2005.0019

Gasche, J. A., & Goel, A. (2012). Epigenetic mechanisms in oral carcinogenesis. *Future Oncol, 8*(11), 1407-1425. doi:10.2217/fon.12.138

Gil-Ad, I., Shtaif, B., Levkovitz, Y., Nordenberg, J., Taler, M., Korov, I., & Weizman, A. (2006). Phenothiazines induce apoptosis in a B16 mouse melanoma cell line and attenuate in vivo melanoma tumor growth. *Oncol Rep, 15*(1), 107-112.

Gillison, M. L., Trotti, A. M., Harris, J., Eisbruch, A., Harari, P. M., Adelstein, D. J., Le, Q. T. (2019). Radiotherapy plus cetuximab or cisplatin in human papillomavirus-positive oropharyngeal cancer (NRG Oncology RTOG 1016): a randomised, multicentre, non-inferiority trial. *Lancet, 393*(10166), 40-50. doi:10.1016/s0140-6736(18)32779-x

Gong, F. R., Wu, M. Y., Shen, M., Zhi, Q., Xu, Z. K., Wang, R., Li, W. (2015). PP2A inhibitors arrest G2/M transition through JNK/Sp1- dependent down-regulation of CDK1 and autophagy-dependent up-regulation of p21. *Oncotarget, 6*(21), 18469-18483. doi:10.18632/oncotarget.4063

Gupta, S. C., Sung, B., Prasad, S., Webb, L. J., & Aggarwal, B. B. (2013). Cancer drug discovery by repurposing: teaching new tricks to old dogs. *Trends Pharmacol Sci, 34*(9), 508-517. doi:10.1016/j.tips.2013.06.005

Gutierrez, A., Pan, L., Groen, R. W. J., Baleydier, F., Kentsis, A., Marineau, J., Aster, J. C. (2014). Phenothiazines induce PP2A-mediated apoptosis in T cell acute lymphoblastic leukemia. *The Journal of Clinical Investigation, 124*(2), 644-655. doi:10.1172/JCI65093

Haddad, R. I., & Shin, D. M. (2008). Recent advances in head and neck cancer. *N Engl J Med, 359*(11), 1143-1154. doi:10.1056/NEJMra0707975

Hanahan, D., & Weinberg, R. A. (2011). Hallmarks of cancer: the next generation. *Cell, 144*(5), 646-674. doi:10.1016/j.cell.2011.02.013

Hardie, D. G. (2003). Minireview: the AMP-activated protein kinase cascade: the key sensor of cellular energy status. *Endocrinology, 144*(12), 5179-5183. doi:10.1210/en.2003-0982

Hashibe, M., Brennan, P., Benhamou, S., Castellsague, X., Chen, C., Curado, M. P., Boffetta, P. (2007). Alcohol drinking in never users of tobacco, cigarette smoking in never drinkers, and the risk of head and neck cancer: pooled analysis in the International Head and Neck Cancer Epidemiology Consortium. *J Natl Cancer Inst, 99*(10), 777-789. doi:10.1093/jnci/djk179

Hennessey, P. T., Westra, W. H., & Califano, J. A. (2009). Human papillomavirus and head and neck squamous cell carcinoma: recent evidence and clinical implications. *J Dent Res, 88*(4), 300-306. doi:10.1177/0022034509333371

Ho, W. S., Feldman, M. J., Maric, D., Amable, L., Hall, M. D., Feldman, G. M., Heiss, J. D. (2016). PP2A inhibition with LB100 enhances cisplatin cytotoxicity and overcomes cisplatin resistance in medulloblastoma cells. *Oncotarget, 7*(11), 12447-12463. doi:10.18632/oncotarget.6970

Horman, S., Browne, G., Krause, U., Patel, J., Vertommen, D., Bertrand, L., Rider, M. (2002). Activation of AMP-activated protein kinase leads to the phosphorylation of elongation factor 2 and an inhibition of protein synthesis. *Curr Biol, 12*(16), 1419-1423.

IQVIA Global Oncology Trends. (2019). Retrieved from IQVIA Institute Report: https://www.iqvia.com/insights/the-iqvia-institute/reports/global-oncology-trends-2019

Jiang, X., Ye, J., Dong, Z., Hu, S., & Xiao, M. (2019). Novel genetic alterations and their impact on target therapy response in head and neck squamous cell carcinoma. *Cancer Manag Res, 11*, 1321-1336. doi:10.2147/cmar.S187780

Kaiser, J. (2011). Biomedicine. NIH's secondhand shop for tried-and-tested drugs. *Science, 332*(6037), 1492. doi:10.1126/science.332.6037.1492

Kiely, M., & Kiely, P. A. (2015). PP2A: The Wolf in Sheep's Clothing? *Cancers (Basel), 7*(2), 648-669. doi:10.3390/cancers7020648

Kim, J., Koo, B. K., & Knoblich, J. A. (2020). Human organoids: model systems for human biology and medicine. *Nat Rev Mol Cell Biol, 21*(10), 571-584. doi:10.1038/s41580-020-0259-3

King, D. J. (1998). Drug treatment of the negative symptoms of schizophrenia. *Eur Neuropsychopharmacol, 8*(1), 33-42. doi:10.1016/s0924-977x(97)00041-2

Koskinen, W. J., Chen, R. W., Leivo, I., Mäkitie, A., Bäck, L., Kontio, R., Aaltonen, L. M. (2003). Prevalence and physical status of human papillomavirus in squamous cell carcinomas of the head and neck. *Int J Cancer, 107*(3), 401-406. doi:10.1002/ijc.11381

Kuzu, O. F., Gowda, R., Noory, M. A., & Robertson, G. P. (2017). Modulating cancer cell survival by targeting intracellular cholesterol transport. *Br J Cancer, 117*(4), 513-524. doi:10.1038/bjc.2017.200

Lee, W. Y., Lee, W. T., Cheng, C. H., Chen, K. C., Chou, C. M., Chung, C. H., Lin, C. W. (2015). Repositioning antipsychotic chlorpromazine for treating colorectal cancer by inhibiting sirtuin 1. *Oncotarget, 6*(29), 27580-27595. doi:10.18632/oncotarget.4768

Leemans, C. R., Braakhuis, B. J., & Brakenhoff, R. H. (2011). The molecular biology of head and neck cancer. *Nat Rev Cancer, 11*(1), 9-22. doi:10.1038/nrc2982

Leemans, C. R., Snijders, P. J. F., & Brakenhoff, R. H. (2018). The molecular landscape of head and neck cancer. *Nat Rev Cancer, 18*(5), 269-282. doi:10.1038/nrc.2018.11

Liang, Y., Lin, S. Y., Brunicardi, F. C., Goss, J., & Li, K. (2009). DNA damage response pathways in tumor suppression and cancer treatment. *World J Surg, 33*(4), 661-666. doi:10.1007/s00268-008-9840-1

Lippman, S. M., & Hong, W. K. (2001). Molecular markers of the risk of oral cancer. *N Engl J Med, 344*(17), 1323-1326. doi:10.1056/nejm200104263441710

Mazhar, S., Taylor, S. E., Sangodkar, J., & Narla, G. (2019). Targeting PP2A in cancer: Combination therapies. *Biochim Biophys Acta Mol Cell Res, 1866*(1), 51-63. doi:10.1016/j.bbamcr.2018.08.020

Mehanna, H., Paleri, V., West, C. M., & Nutting, C. (2011). Head and neck cancer-part 1: epidemiology, presentation, and preservation. *Clin Otolaryngol, 36*(1), 65-68. doi:10.1111/j.1749-4486.2010.02231.x

Mehanna, H., Rischin, D., Wong, S. J., Gregoire, V., Ferris, R., Waldron, J., Porceddu, S. (2020). De-Escalation After DE-ESCALATE and RTOG 1016: A Head and

Neck Cancer InterGroup Framework for Future De-Escalation Studies. *J Clin Oncol, 38*(22), 2552-2557. doi:10.1200/jco.20.00056

O'Connor, C. M., Perl, A., Leonard, D., Sangodkar, J., & Narla, G. (2018). Therapeutic targeting of PP2A. *Int J Biochem Cell Biol, 96*, 182-193. doi:10.1016/j.biocel.2017.10.008

Palanichamy, K., Kanji, S., Gordon, N., Thirumoorthy, K., Jacob, J. R., Litzenberg, K. T., Chakravarti, A. (2017). NNMT Silencing Activates Tumor Suppressor PP2A, Inactivates Oncogenic STKs, and Inhibits Tumor Forming Ability. *Clin Cancer Res, 23*(9), 2325-2334. doi:10.1158/1078-0432.Ccr-16-1323

Pastor, D. M., Poritz, L. S., Olson, T. L., Kline, C. L., Harris, L. R., Koltun, W. A., Irby, R. B. (2010). Primary cell lines: false representation or model system? a comparison of four human colorectal tumors and their coordinately established cell lines. *Int J Clin Exp Med, 3*(1), 69-83.

Pollak, M. (2014). Overcoming Drug Development Bottlenecks With Repurposing: Repurposing biguanides to target energy metabolism for cancer treatment. *Nat Med, 20*(6), 591-593. doi:10.1038/nm.3596

Pu, X., Kamendulis, L. M., & Klaunig, J. E. (2009). Acrylonitrile-induced oxidative stress and oxidative DNA damage in male Sprague-Dawley rats. *Toxicol Sci, 111*(1), 64-71. doi:10.1093/toxsci/kfp133

Pulkoski-Gross, A., Li, J., Zheng, C., Li, Y., Ouyang, N., Rigas, B., Cao, J. (2015). Repurposing the antipsychotic trifluoperazine as an antimetastasis agent. *Mol Pharmacol, 87*(3), 501-512. doi:10.1124/mol.114.096941

Puram, S. V., & Rocco, J. W. (2015). Molecular Aspects of Head and Neck Cancer Therapy. *Hematol Oncol Clin North Am, 29*(6), 971-992. doi:10.1016/j.hoc.2015.07.003

Purdue, M. P., Hashibe, M., Berthiller, J., La Vecchia, C., Dal Maso, L., Herrero, R., Hayes, R. B. (2009). Type of alcoholic beverage and risk of head and neck cancer--a pooled analysis within the INHANCE Consortium. *Am J Epidemiol, 169*(2), 132-142. doi:10.1093/aje/kwn306

Ramaswamy, K., Spitzer, B., & Kentsis, A. (2015). Therapeutic Re-Activation of Protein Phosphatase 2A in Acute Myeloid Leukemia. *Front Oncol, 5*, 16. doi:10.3389/fonc.2015.00016

Rice, L. M., Donigan, M., Yang, M., Liu, W., Pandya, D., Joseph, B. K., Nickels, J. T., Jr. (2014). Protein phosphatase 2A (PP2A) regulates low density lipoprotein uptake through regulating sterol response element-binding protein-2 (SREBP-2) DNA binding. *J Biol Chem, 289*(24), 17268-17279. doi:10.1074/jbc.M114.570390

Rikiishi, H., Shinohara, F., Sato, T., Sato, Y., Suzuki, M., & Echigo, S. (2007). Chemosensitization of oral squamous cell carcinoma cells to cisplatin by histone deacetylase inhibitor, suberoylanilide hydroxamic acid. *Int J Oncol, 30*(5), 1181-1188.

Sanchez-Cespedes, M., Esteller, M., Wu, L., Nawroz-Danish, H., Yoo, G. H., Koch, W. M., Sidransky, D. (2000). Gene promoter hypermethylation in tumors and serum of head and neck cancer patients. *Cancer Res, 60*(4), 892-895.

Sangodkar, J., Perl, A., Tohme, R., Kiselar, J., Kastrinsky, D. B., Zaware, N., Narla, G. (2017). Activation of tumor suppressor protein PP2A inhibits KRAS-driven tumor growth. *J Clin Invest, 127*(6), 2081-2090. doi:10.1172/jci89548

Shin, S. Y., Kim, C. G., Kim, S. H., Kim, Y. S., Lim, Y., & Lee, Y. H. (2010). Chlorpromazine activates p21Waf1/Cip1 gene transcription via early growth response-1 (Egr-1) in C6 glioma cells. *Exp Mol Med, 42*(5), 395-405. doi:10.3858/emm.2010.42.5.041

Shin, S. Y., Lee, K. S., Choi, Y. K., Lim, H. J., Lee, H. G., Lim, Y., & Lee, Y. H. (2013). The antipsychotic agent chlorpromazine induces autophagic cell death by inhibiting the Akt/mTOR pathway in human U-87MG glioma cells. *Carcinogenesis, 34*(9), 2080-2089. doi:10.1093/carcin/bgt169

Siddik, Z. H. (2003). Cisplatin: mode of cytotoxic action and molecular basis of resistance. *Oncogene, 22*(47), 7265-7279. doi:10.1038/sj.onc.1206933

Sleire, L., Forde, H. E., Netland, I. A., Leiss, L., Skeie, B. S., & Enger, P. O. (2017). Drug repurposing in cancer. *Pharmacol Res, 124*, 74-91. doi:10.1016/j.phrs.2017.07.013

Suzuki, M., Shinohara, F., Nishimura, K., Echigo, S., & Rikiishi, H. (2007). Epigenetic regulation of chemosensitivity to 5-fluorouracil and cisplatin by zebularine in oral squamous cell carcinoma. *Int J Oncol, 31*(6), 1449-1456.

Tsuji, S., Yabe, R., Usui, T., Mizuno, T., Ohama, T., & Sato, K. (2016). Anti-tumor effects of perphenazine on canine lymphoma. *J Vet Med Sci, 78*(8), 1293-1298. doi:10.1292/jvms.15-0707

Uddin, M. H., Pimentel, J. M., Chatterjee, M., Allen, J. E., Zhuang, Z., & Wu, G. S. (2020). Targeting PP2A inhibits the growth of triple-negative breast cancer cells. *Cell Cycle, 19*(5), 592-600. doi:10.1080/15384101.2020.1723195

Vokes, E. E., Agrawal, N., & Seiwert, T. Y. (2015). HPV-Associated Head and Neck Cancer. *JNCI: Journal of the National Cancer Institute, 107*(12). doi:10.1093/jnci/djv344

Weissenrieder, J. S., Neighbors, J. D., Mailman, R. B., & Hohl, R. J. (2019). Cancer and the Dopamine D2 Receptor: A Pharmacological Perspective. *J Pharmacol Exp Ther, 370*(1), 111-126. doi:10.1124/jpet.119.256818

Winn, D. M. (1992). Smokeless tobacco and aerodigestive tract cancers: recent research directions. *Adv Exp Med Biol, 320*, 39-46. doi:10.1007/978-1-4615-3468-6_6

Wlodarchak, N., & Xing, Y. (2016). PP2A as a master regulator of the cell cycle. *Crit Rev Biochem Mol Biol, 51*(3), 162-184. doi:10.3109/10409238.2016.1143913

Yang, J., Wei, J., Wu, Y., Wang, Z., Guo, Y., Lee, P., & Li, X. (2015). Metformin induces ER stress-dependent apoptosis through miR-708-5p/NNAT pathway in prostate cancer. *Oncogenesis, 4*, e158. doi:10.1038/oncsis.2015.18

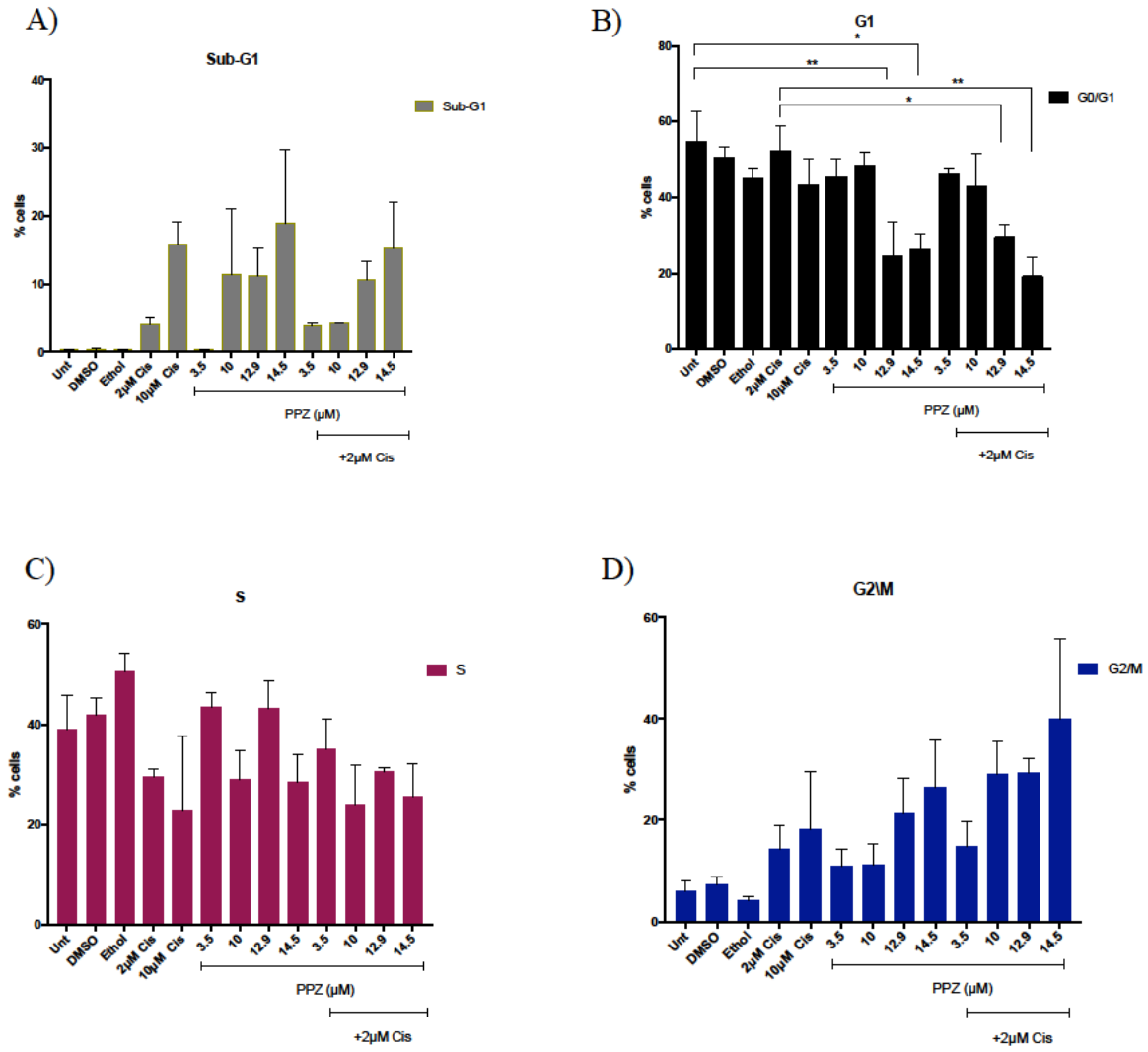
Zhelev, Z., Ohba, H., Bakalova, R., Hadjimitova, V., Ishikawa, M., Shinohara, Y., & Baba, Y. (2004). Phenothiazines suppress proliferation and induce apoptosis in cultured leukemic cells without any influence on the viability of normal lymphocytes. Phenothiazines and leukemia. *Cancer Chemother Pharmacol, 53*(3), 267-275. doi:10.1007/s00280-003-0738-1

Ziemann, F., Arenz, A., Preising, S., Wittekindt, C., Klussmann, J. P., Engenhart-Cabillic, R., & Wittig, A. (2015). Increased sensitivity of HPV-positive head and neck cancer cell lines to x-irradiation ± Cisplatin due to decreased expression of E6 and E7 oncoproteins and enhanced apoptosis. *Am J Cancer Res, 5*(3), 1017-1031.

9. Appendix

Supplementary Table 1: RNA-seq data analysis (data collected from Kuzu et al. (2017)**)**

RNA-Seq enrichment analysis		
pathway	P adj	Tool
mitotic cell cycle	1.562×10^{-46}	GO:BP
cell cycle	3.196×10^{-45}	GO:BP
mitotic cell cycle process	1.765×10^{-42}	GO:BP
cell cycle process	4.986×10^{-36}	GO:BP
regulation of cell cycle	7.885×10^{-23}	GO:BP
cell cycle phase transition	1.184×10^{-21}	GO:BP
DNA replication	1.397×10^{-16}	GO:BP
regulation of cell cycle process	2.745×10^{-16}	GO:BP
cell cycle G2/M pase transition	2.745×10^{-16}	GO:BP
cell cycle	3.607×10^{-13}	KEGG
DNA replication	2.704×10^{-10}	KEGG
cell cycle	2.540×10^{-42}	REAC
cell cycle,Mitotic	1.272×10^{-38}	REAC
M Phase	7.383×10^{-23}	REAC
G1/S transition	2.061×10^{-12}	REAC
cell cycle	1.020×10^{-10}	WP



Supplementary Figure 1: Cell cycle analysis in Cal27 cell lines with PPZ treatment modified from Figure 11 indicating that PPZ promotes G1 to S transition in cell cycle (N=3). A)Sub-G1 phase histogram, B) G1 phase histogram, C) S phase histogram, D) G2/M phase. Statistical significance calculated by a two-way ANOVA followed by Dunnett's multiple comparisons test. *Stars indicates P-values on the graphs as follows: *= p<0.05; **=p<0.01.